A Perspective on the 40-Year History of FDTD Computational Electrodynamics

Allen Taflove, Professor

Department of Electrical Engineering and Computer Science
Northwestern University, Evanston, IL 60208

Presented at:

Applied Computational Electromagnetics Society (ACES) Conference
Miami, Florida

March 15, 2006

Paper Number 1: Kane Yee
IEEE AP-S Transactions, May 1966

Numerical Solution of Initial Boundary Value Problems Involving Maxwell's Equations In Isotropic Media

KANE S. YEE

Abstract—Maxwell's equations are replaced by a set of finite difference equations. It is shown that if one chooses the field points appropriately, the set of finite difference equations is applicable for a boundary condition involving perfectly conducting surfaces. An example is given of the scattering of an electromagnetic pulse by a perfectly conducting cylinder.

obstacle is moderately large compared to that of an incoming wave.

A set of finite difference equations for the system of partial differential equations will be introduced in the early part of this paper. We shall then show that with an

2441 citations as of March 7, 2006 (Source: ISI Web of Science)

Yearly FDTD-Related Publications

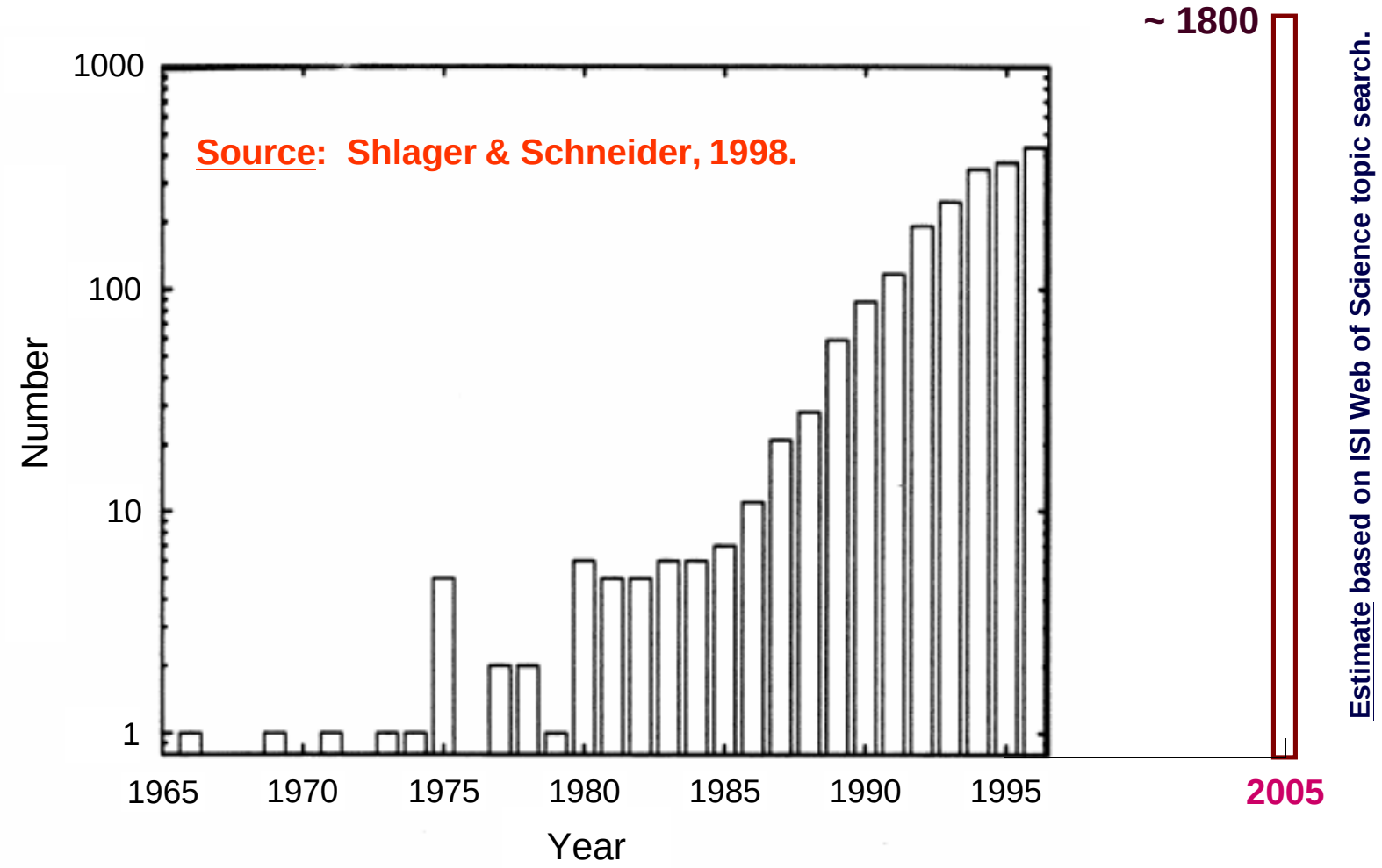

My First Paper: IEEE MTT, Aug. 1975

Numerical Solution of Steady-State Electromagnetic Scattering Problems Using the Time-Dependent Maxwell's Equations

ALLEN TAFLOVE AND MORRIS E. BRODWIN, SENIOR MEMBER, IEEE

***Abstract*—A numerical method is described for the solution of the electromagnetic fields within an arbitrary dielectric scatterer of the order of one wavelength in diameter. The method treats the irradiation of the scatterer as an initial value problem. At $t = 0$, a plane-wave source of frequency f is assumed to be turned on. The diffraction of waves from this source is modeled by repeatedly solving a finite-difference analog of the time-dependent Maxwell's equations. Time stepping is continued until sinusoidual steady-state field values are observed at all points within the scatterer. The envelope of the standing wave is taken as the steady-state scattered field. As an example of this method, the computed results for a dielectric cylinder scatterer are presented. An error of less than ±10 percent in locating and evaluating the standing-wave peaks within the cylinder is achieved for a program execution time of 1 min. The extension of this method to the solution of the fields within three-dimensional dielectric scatterers is outlined.**

microwaves upon living tissue. Exact analytical solutions are obtained only for simple scatterers like the sphere and the circular cylinder, which may be solved using separation of variables. For complicated scatterers like most body organs, we must resort to some numerical method if an accurate model is to be examined.

The computer techniques relevant to this problem that have appeared in the literature may be called, as a class, frequency-domain methods. These methods are based upon the assumption of an exp $(j2\pi ft)$ time dependence in the fundamental Maxwell's equations. In general, methods of this type derive a set of linear equations for either field variables or field expansion coefficients, and then solve the linear system with a suitable matrix-inversion scheme.

My Second Paper: IEEE MTT, Nov. 1975

Computation of the Electromagnetic Fields and Induced Temperatures Within a Model of the Microwave-Irradiated Human Eye

ALLEN TAFLOVE AND MORRIS E. BRODWIN, SENIOR MEMBER, IEEE

Abstract—**The electromagnetic fields within a detailed model of the human eye and its surrounding bony orbit are calculated for two different frequencies of plane-wave irradiation: 750 MHz and 1.5 GHz. The computation is performed with a finite-difference algorithm for the time-dependent Maxwell's equations, carried out to the sinusoidal steady state. The heating potential, derived from the square of the electric field, is used to calculate the temperatures induced within the eyeball of the model. This computation is performed with the implicit alternating-direction (IAD) algorithm for the heat conduction equation. Using an order-of-magnitude estimate of the heat-sinking capacity of the retinal blood supply, it is determined that a hot spot exceeding 40.4°C occurs at the center of the model eyeball at an incident power level of 100 mW/cm² at 1.5 GHz.**

likely thermal [5]. A standard for human exposure, based upon such animal experimentation, has been published [6].

The use of animal experimentation to establish a human exposure standard for microwave radiation implies that the anatomy, physiology, and electromagnetic environment of the test animals can be related to that of humans. However, several elements of this relation remain unclear. In particular, the role of tissue structure in determining microwave absorption may be significant. We know that electromagnetic wave absorption in a lossy dielectric scatterer is a function of its shape and dimensions. It is

Coining of "FDTD": IEEE EMC, Aug. 1980

IEEE TRANSACTIONS ON ELECTROMAGNETIC COMPATIBILITY, VOL. EMC-22, NO. 3, AUGUST 1980

Application of the Finite-Difference Time-Domain Method to Sinusoidal Steady-State Electromagnetic-Penetration Problems

ALLEN TAFLOVE, MEMBER, IEEE

Abstract—**A numerical method for predicting the sinusoidal steady-state electromagnetic fields penetrating an arbitrary dielectric or conducting body is described here. The method employs the finite-difference time-domain (FD–TD) solution of Maxwell's curl equations implemented on a cubic-unit-cell space lattice. Small air-dielectric loss factors are introduced to improve the lattice truncation conditions and to accelerate convergence of cavity interior fields to the sinusoidal steady state. This method is evaluated with comparison to classical theory, method-of-moment frequency-domain numerical theory, and experimental results via application to a dielectric sphere and a cylindrical metal cavity with an aperture. Results are also given for a missile-like cavity with two different types of apertures illuminated by an axial-incidence plane wave.**

Key Words—**Finite-difference, time-domain, steady-state, plane wave, electromagnetic penetration, apertures, dielectric sphere, cylindrical metal cavity, missile-like cavity.**

modeling approaches. First, it is simple to implement for complicated metal/dielectric structures because arbitrary electrical parameters can be assigned to each lattice cell using a data card deck. Second, its computer memory and running time requirement is not prohibitive for many complex structures of interest. In recent work, the FD–TD method has been shown capable of accurately solving for hundreds of thousands of unknown field components within a few minutes on an array-processing computer. Consistently, a ±1-dB accuracy relative to known analytical and experimental bench marks has been achieved for a variety of dielectric and metal geometries.

The objective of present work is to evaluate the suitability of the FD–TD method to determine the amount of elec-

Timeline: 1966 to 1980

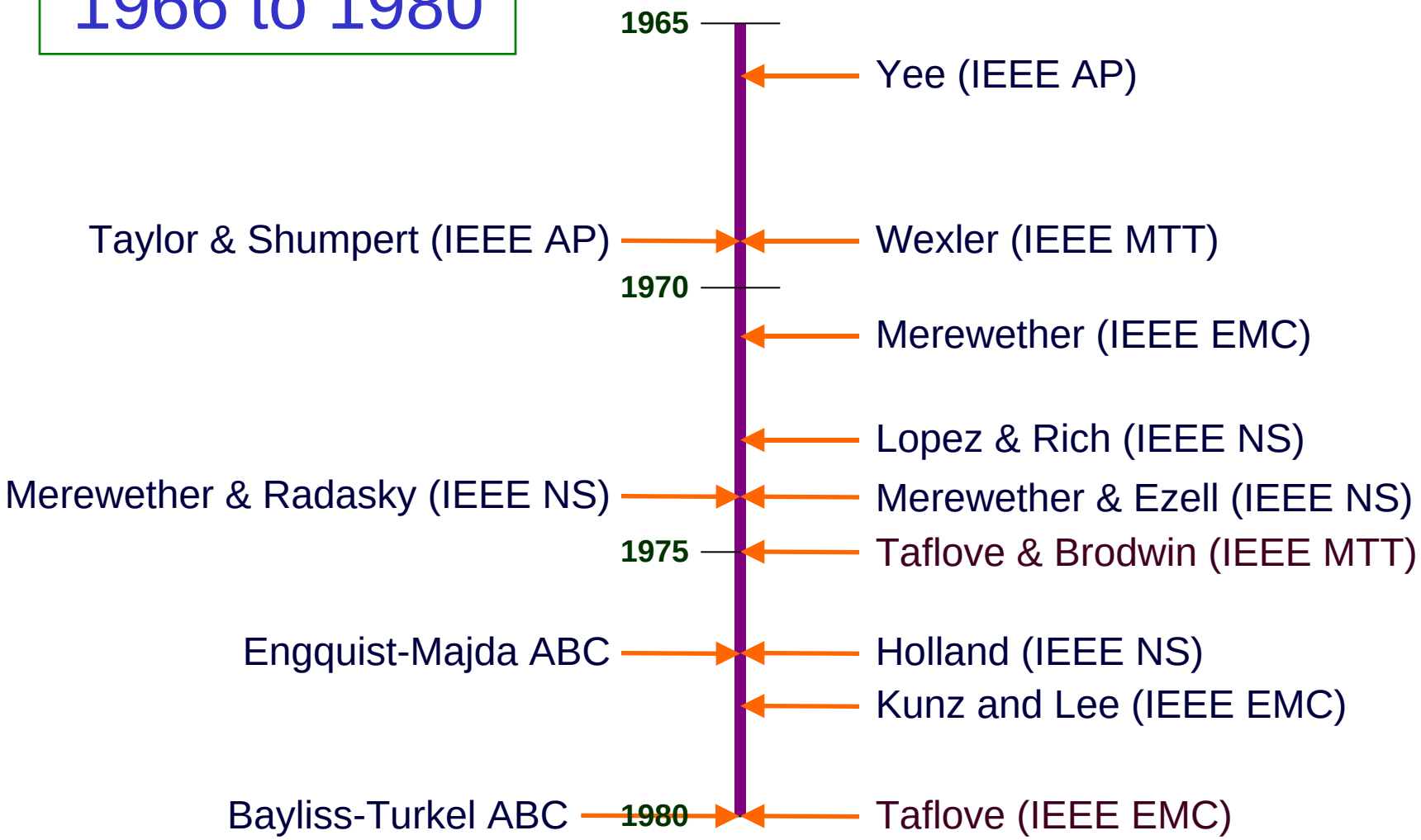

Timeline: 1981 to 1990

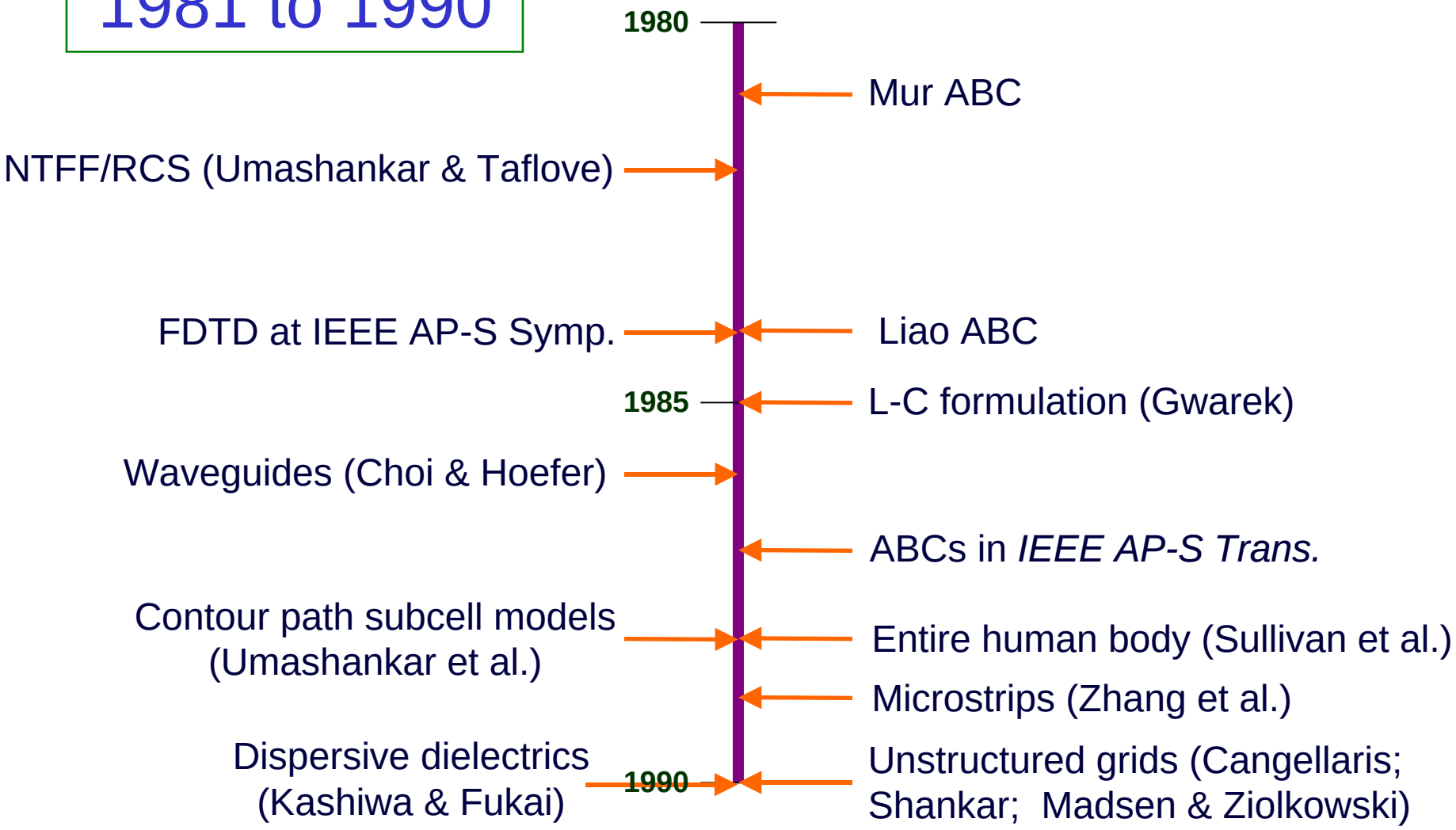

Timeline: 1991 to 1995

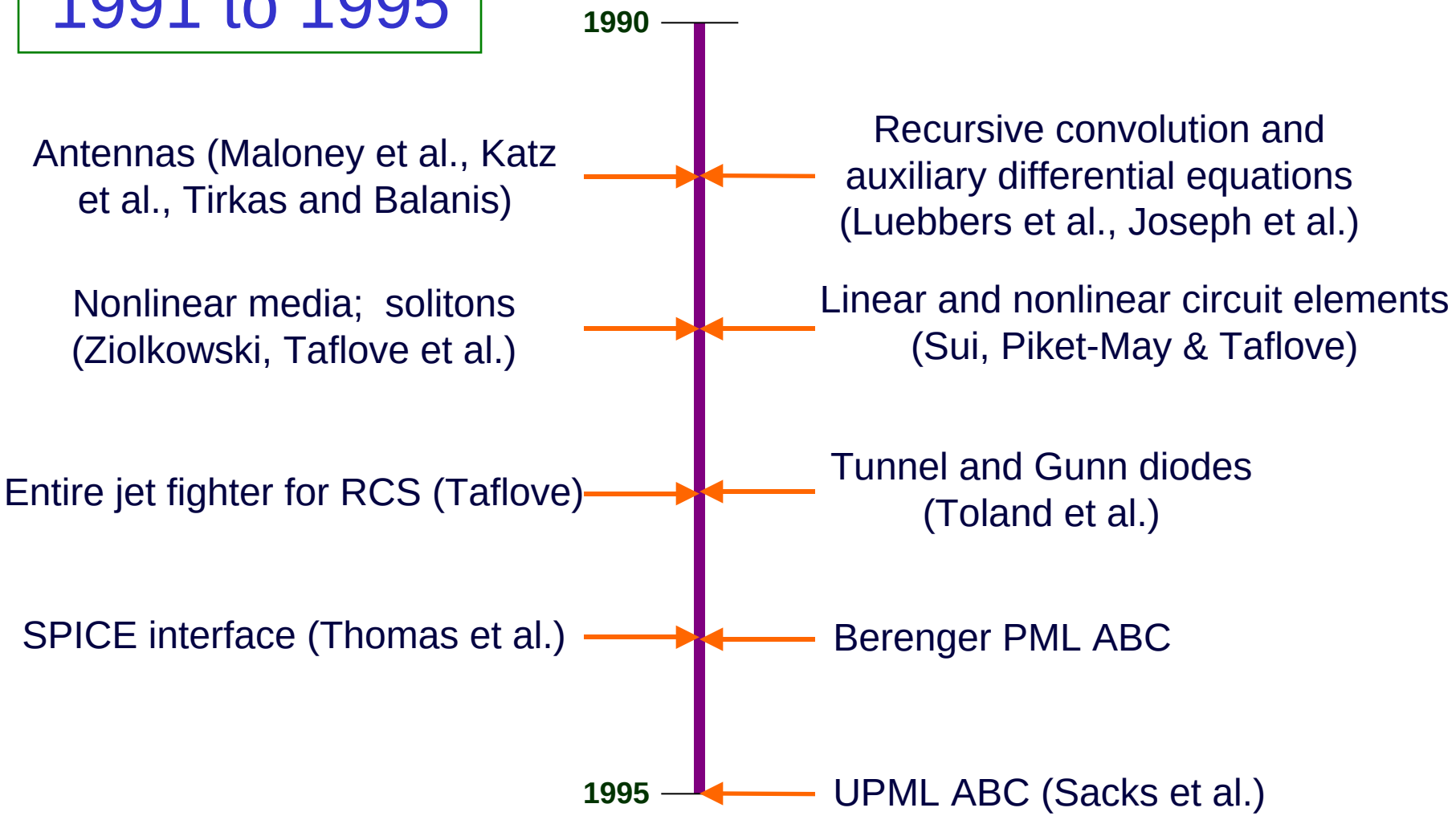

Timeline: 1996 to 2000

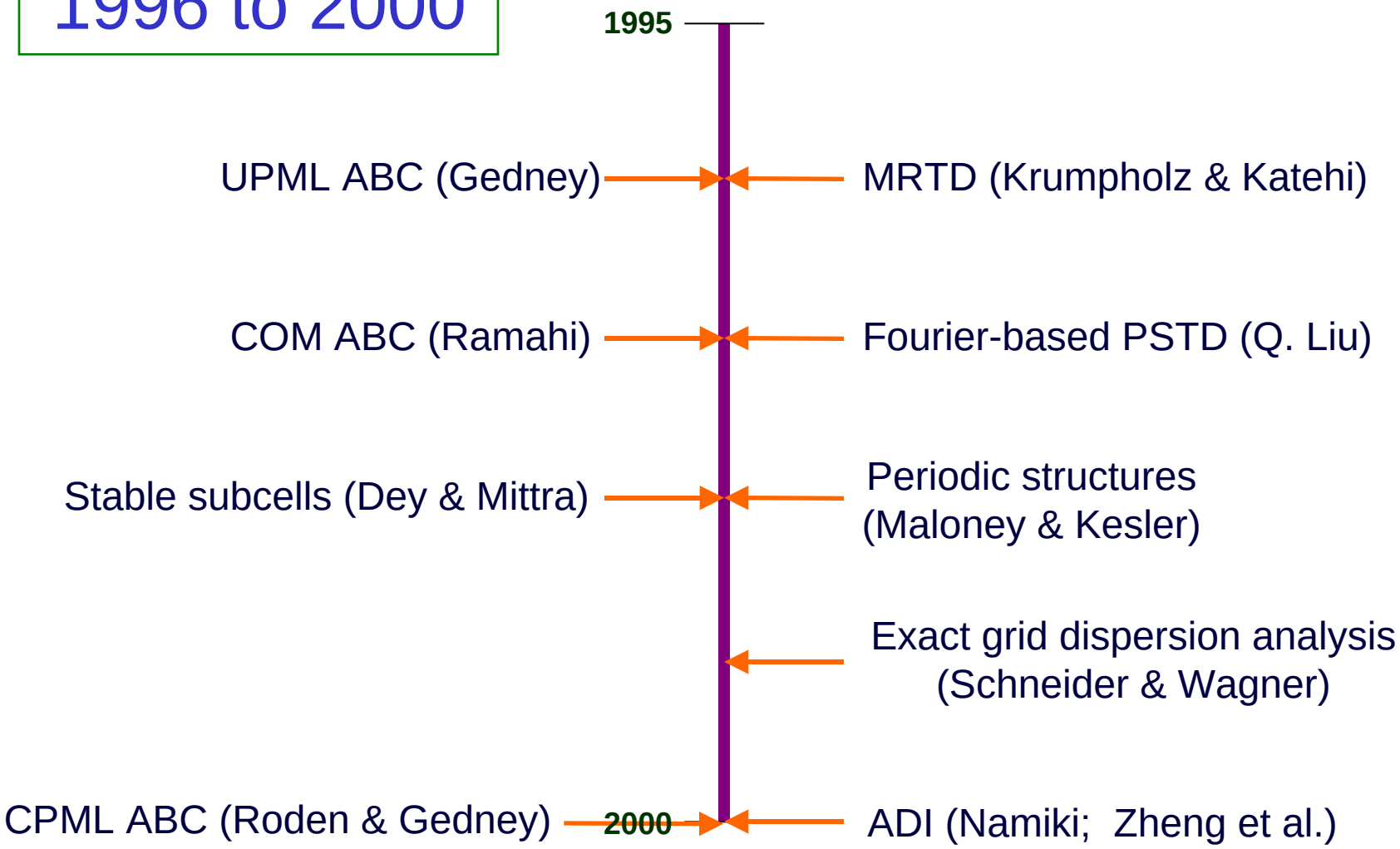

Timeline: 2000 to 2005

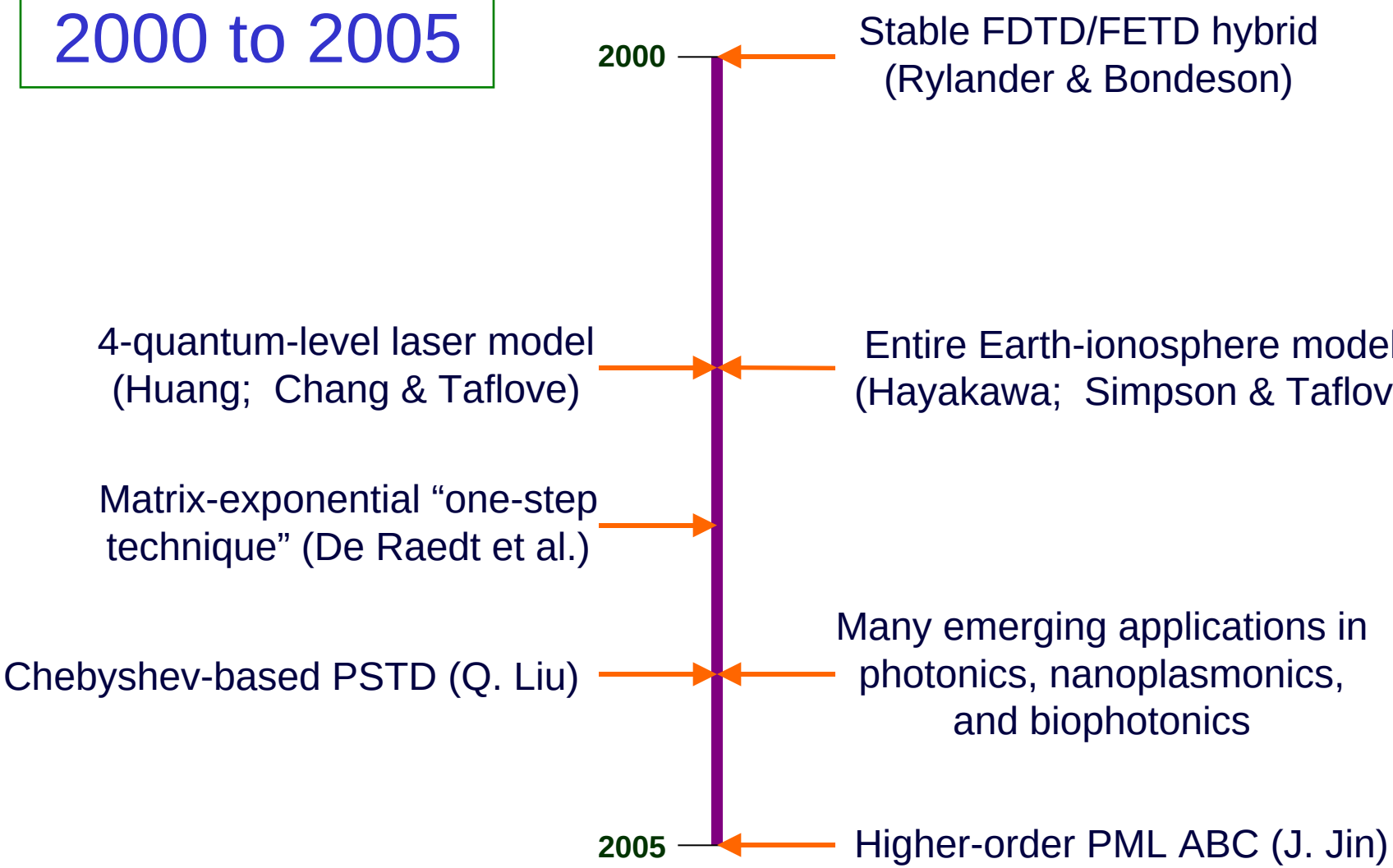

Some Major Technical Paths Since Yee

- Absorbing boundary conditions
- Numerical dispersion
- Numerical stability
- Conforming grids
- Digital signal processing
- Dispersive and nonlinear materials
- Multiphysics

Some Major Technical Paths Since Yee

- Absorbing boundary conditions
  - Engquist-Majda, *Math. Comp*., 1977
  - Bayliss-Turkel, *Com. Pure Appl. Math*., 1980
  - Liao et al., *Scientia Sinica A*, 1984
  - Berenger PML, *1994 JCP*
    - UPML, CPML, higher-order PML

Some Major Technical Paths Since Yee

- Numerical dispersion
  - Schneider and Wagner, *IEEE MGWL*, 1999
  - High-order space differences
  - MRTD (Krumpholz and Katehi, *IEEE MTT*, 1996)
  - PSTD (Q. H. Liu, *1997 IEEE AP-S Symp*.)

Some Major Technical Paths Since Yee

- Numerical stability
  - Taflove & Brodwin, *IEEE MTT*, 1975
  - ADI techniques (Namiki, *IEEE MTT,* 1999; Zheng, Chen, and Zhang, *IEEE MTT*, 2000)
  - One-step Chebyshev method (De Raedt et al., *IEEE AP,* 2003)

Some Major Technical Paths Since Yee

- Conforming grids
  - Locally conforming (Taflove-Umashankar contour path, Dey/Yu-Mittra)
  - Globally conforming (Shankar et al., and Madsen and Ziolkowski, *Electromagnetics*, 1990).
  - Stable hybrid FETD/FDTD (Rylander and Bondeson, *Comput. Phys. Comm*., 2000).

Some Major Technical Paths Since Yee

- Digital signal processing
  - Near-to-far-field transformation (Umashankar and Taflove, *IEEE EMC*, 1982, 1983; Luebbers et al., *IEEE AP*, 1991)
  - Impulse response Fourier transformation and extrapolation
  - Extraction of resonances, possibly degenerate

Some Major Technical Paths Since Yee

- Dispersive and nonlinear materials
  - Isotropic linear dispersions (Debye, Lorentz, Drude characteristics; multiple poles)
  - Anisotropic linear dispersions (magnetized plasmas, ferrites)
  - Nonlinear dispersions, yielding temporal and spatial solitons

Some Major Technical Paths Since Yee

- Multiphysics coupling to Maxwell's equations
  - Charge generation,recombination, and transport in semiconductors
  - Electron transitions between multiple energy levels of atoms, modeling pumping, emission, and stimulated emission processes

Some Interesting Emerging Applications

- Earth / ionosphere models in geophysics
- Wireless personal communications devices
- Ultrawideband microwave detection of early-stage breast cancer
- Ultrahigh-speed bandpass digital interconnects
- Micron / nanometer-scale photonic devices
- Biophotonics, especially optical detection of early stage epithelial cancers

Earth / Ionosphere Models in Geophysics

Earth / Ionosphere Models in Geophysics

- There is a rich history of investigation of ELF and VLF electromagnetic wave propagation within the Earth-ionosphere waveguide.

- Applications:
  - Submarine communications
  - Remote-sensing of lightning and sprites
  - Global temperature change
  - Subsurface structures
  - Potential earthquake precursors

Geodesic Grid

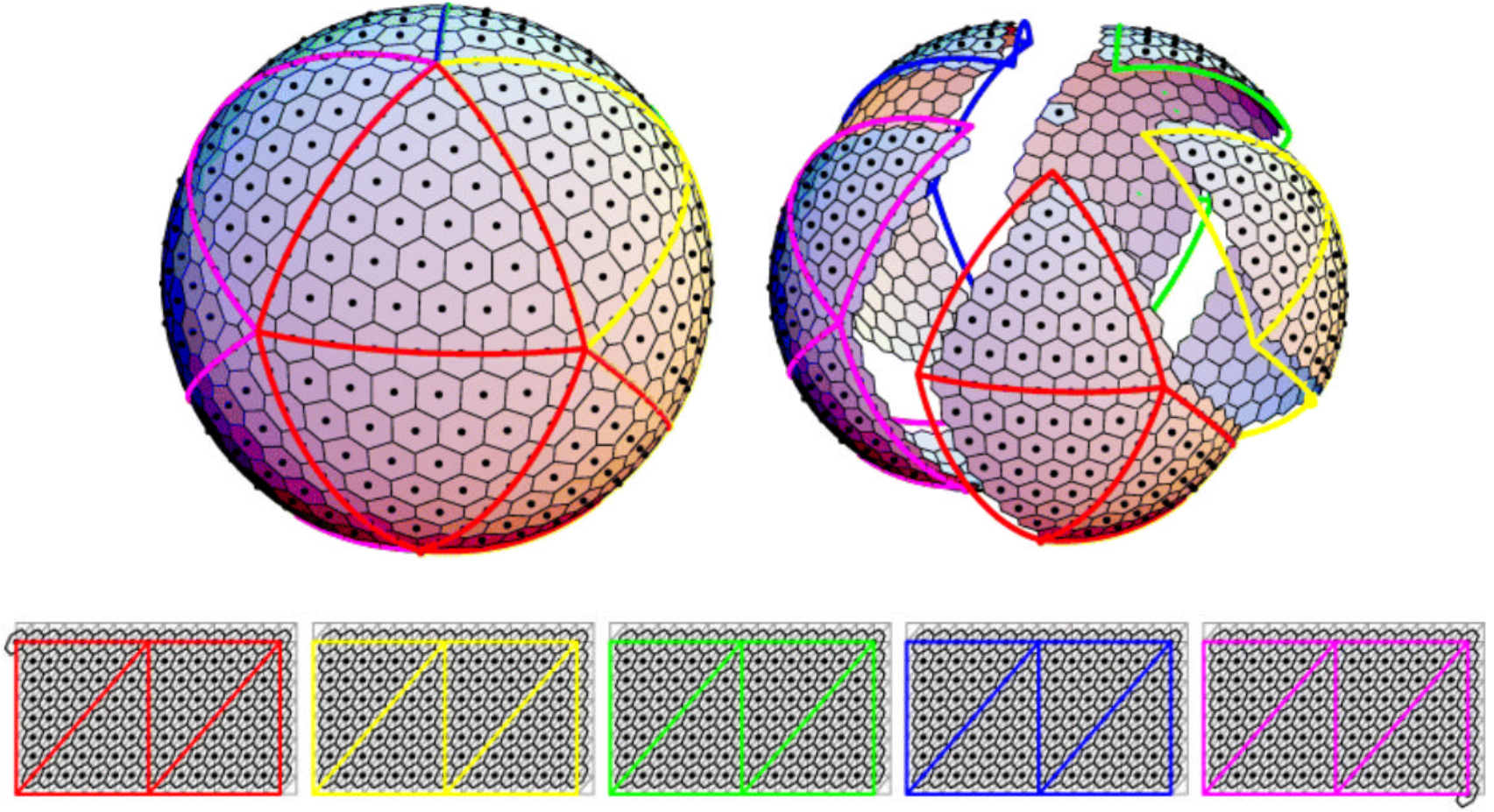

Source: Simpson & Taflove, *IEEE Trans. Antennas and Propagation*, in press.

Snapshots of FDTD-Computed Global Propagation of ELF Electromagnetic Pulse Generated by Vertical Lightning Strike off South America Coast

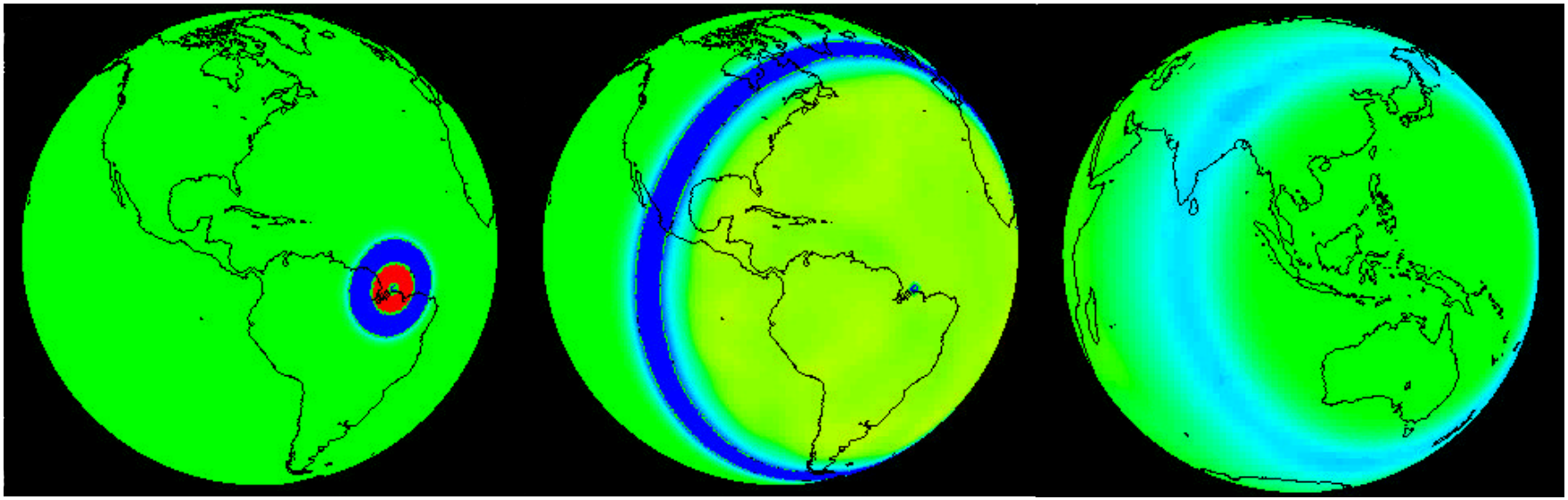

All features of the lithosphere and atmosphere located within ±100 km of sea level are modeled in 3-D with a resolution of approximately 40 × 40 × 5 km.

Detection of an Ionosphere Depression Above Los Angeles (Hypothesized Precursor of a Major Earthquake) Via Illumination by a 76-Hz Pulse from the Former Navy WTF

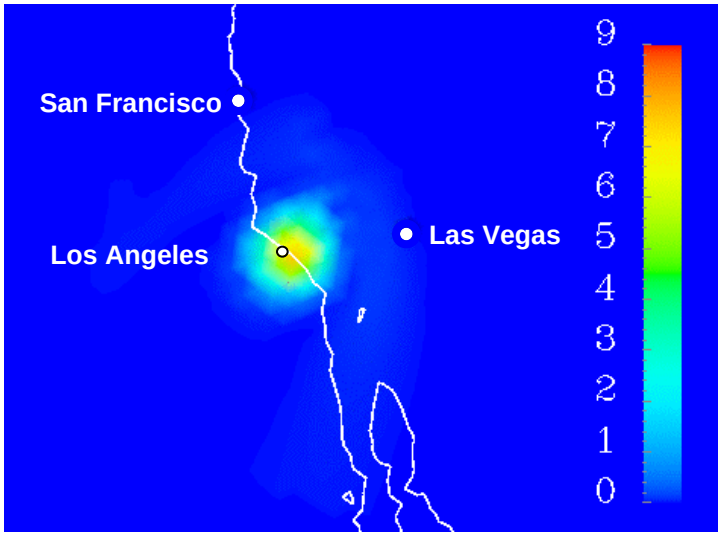

200-km radius

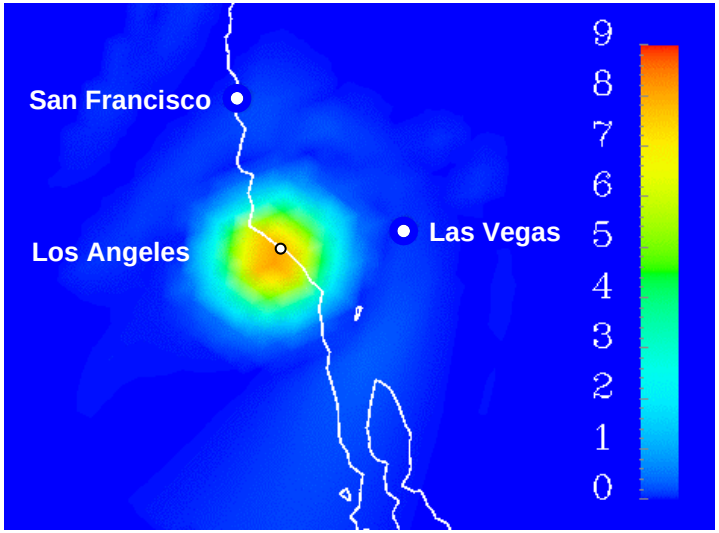

380-km radius

Map of the percent increase in the peak vertical *E*-field power for 20-km deep bowl-shaped ionospheric depressions above downtown Los Angeles.

Source: Simpson & Taflove, *IEEE Geoscience & Remote Sensing Letters*, submitted.

Wireless Personal Communications Devices

Motorola T250 Cellphone

Physical phone

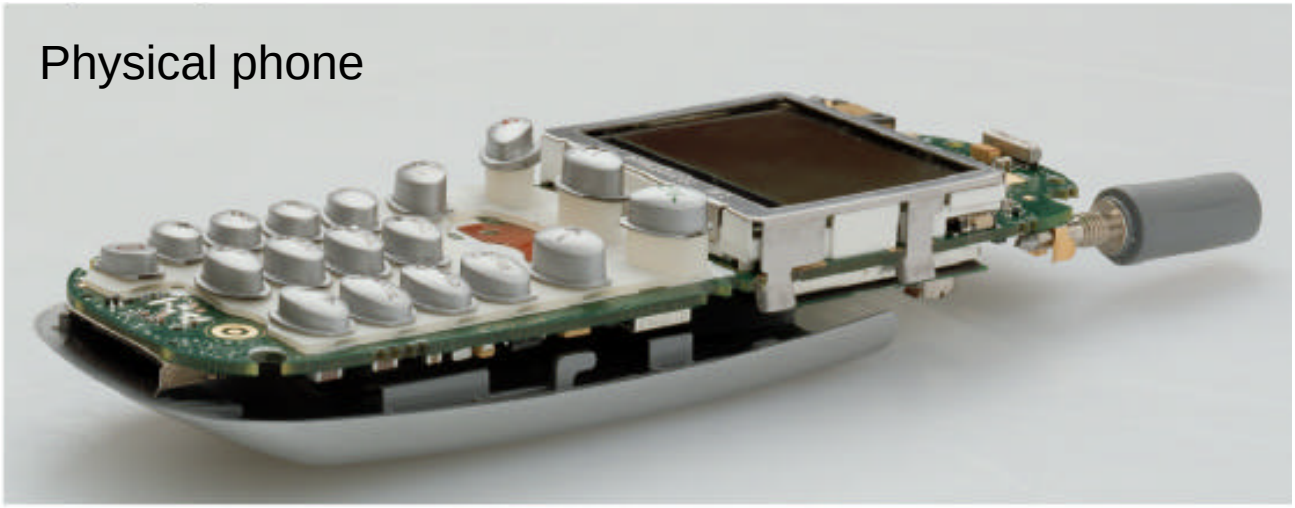

CAD model

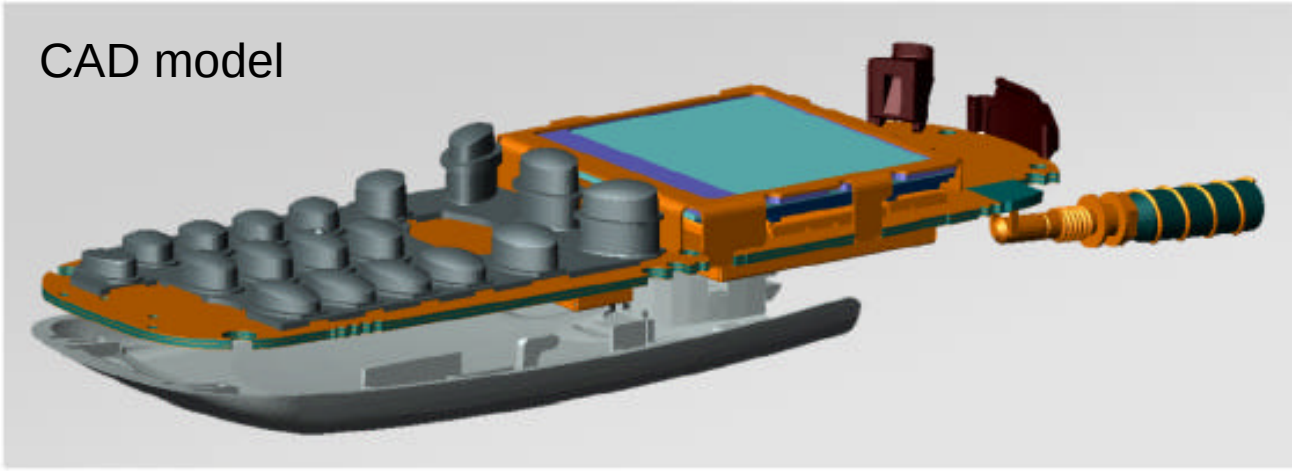

High-resolution FDTD model. The lattice-cell size is as fine as 0.1 mm to resolve individual circuit board layers and the helical antenna.

Source: Chavannes et al., *IEEE Antennas and Propagation Magazine*, Dec. 2003, pp. 52–66.

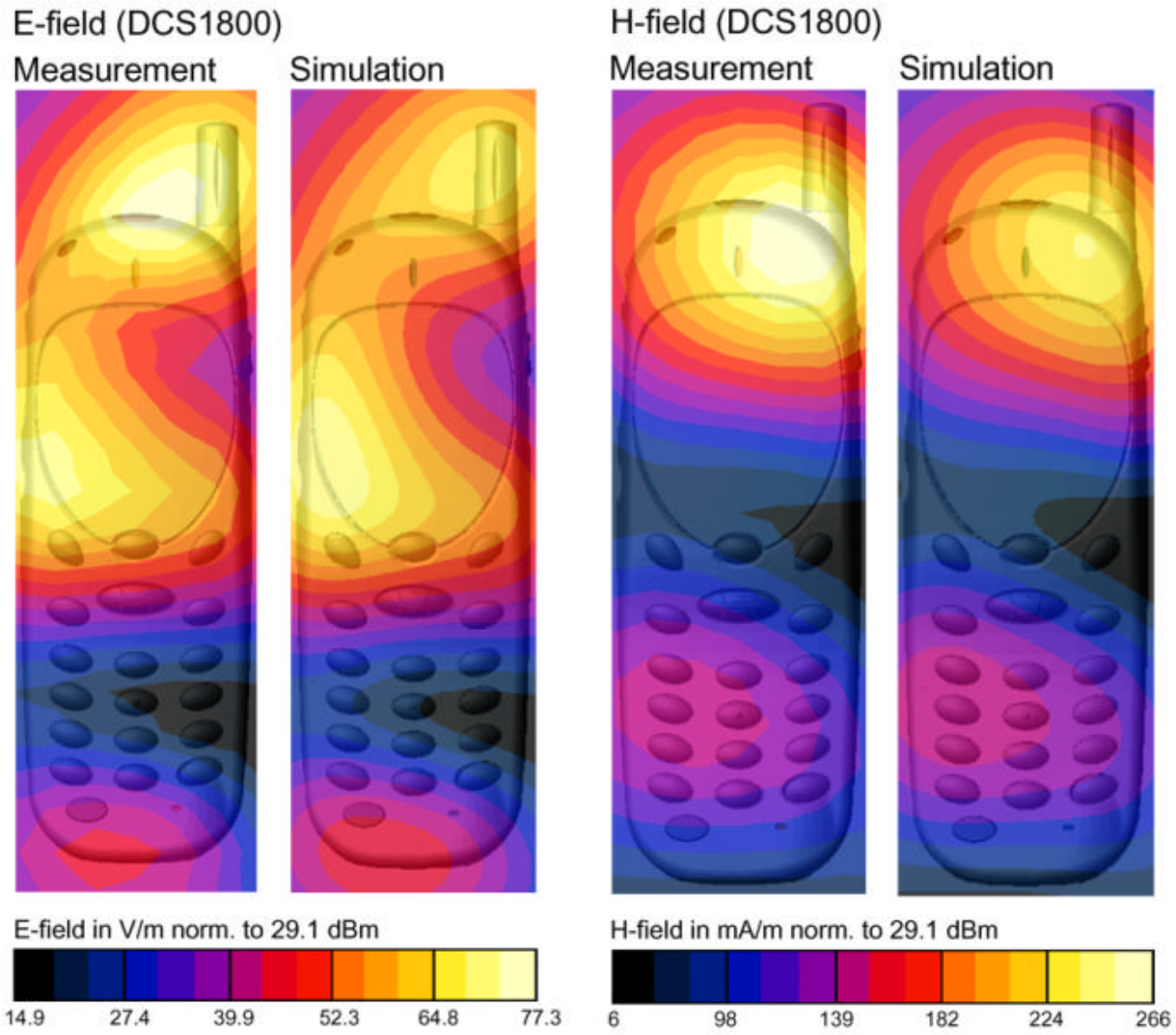

Phone Model Validation at 1.8 GHz

Phantom Head Validation at 1.8 GHz

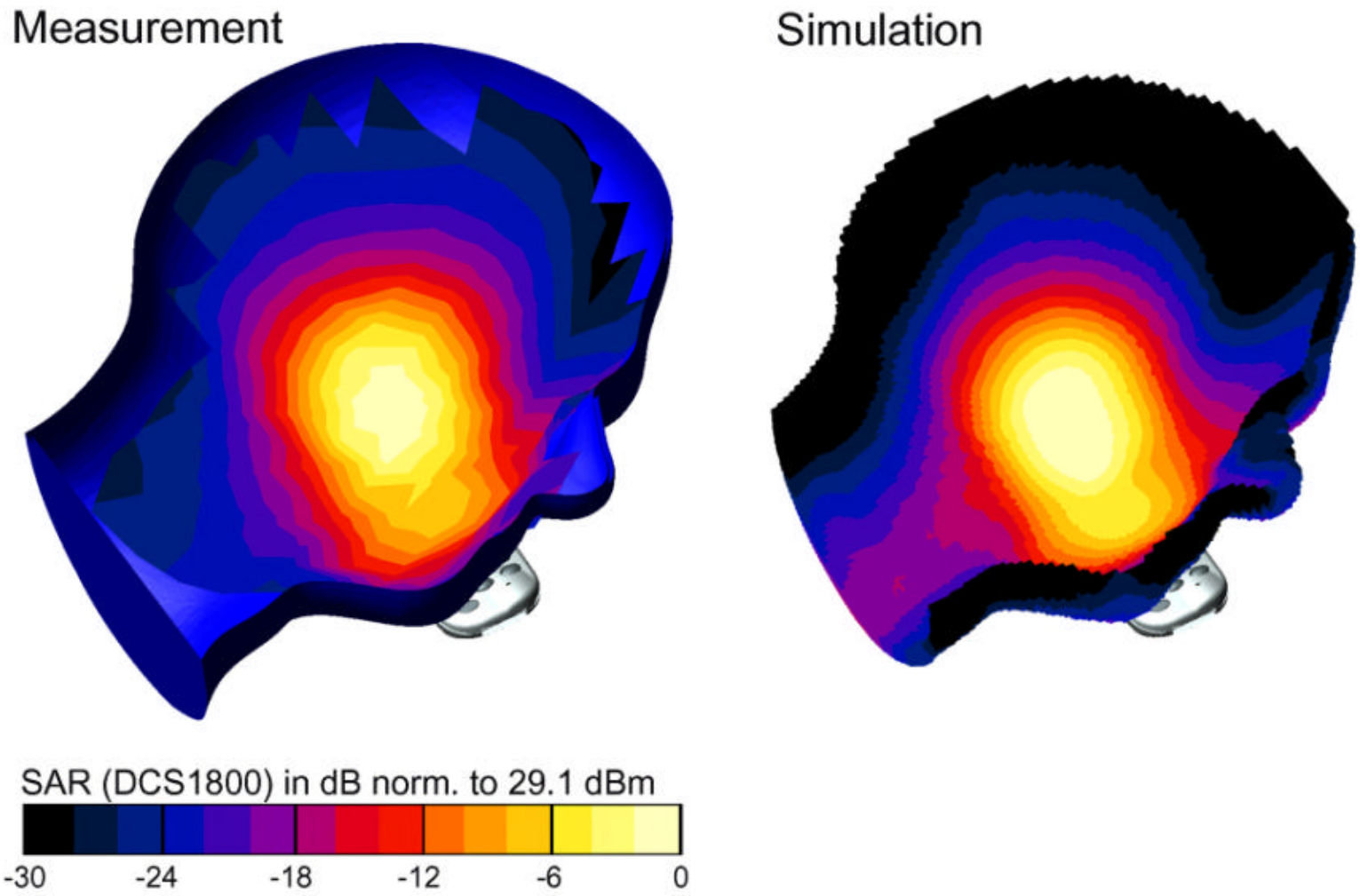

Final Head Model Results

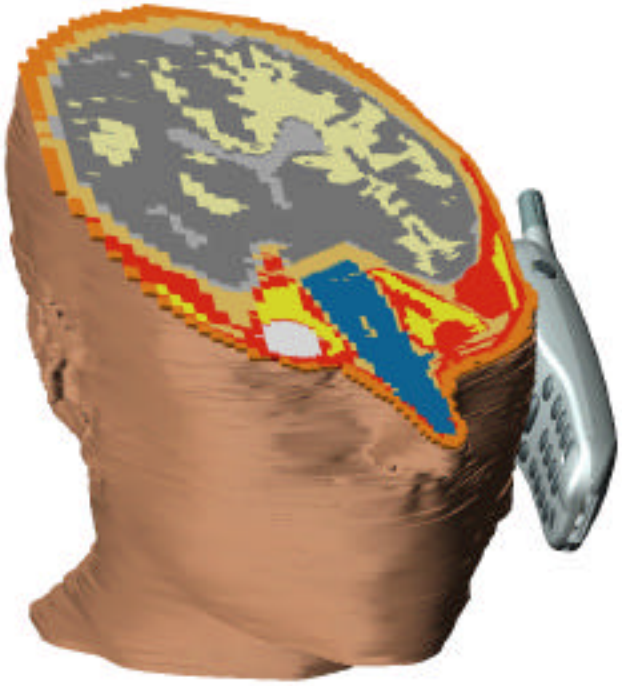

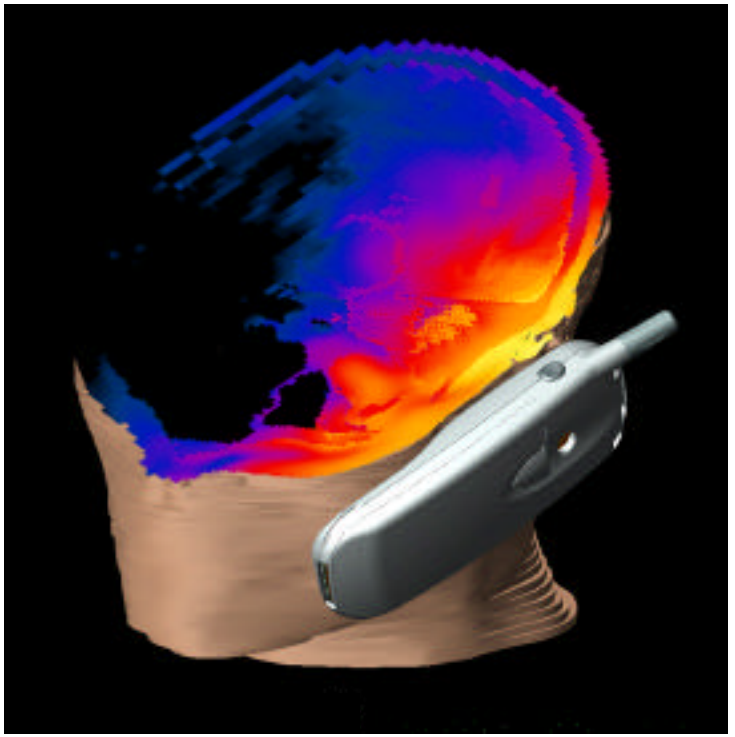

The head model has 121 slices (1-mm thick in the ear region; 3-mm thick elsewhere) having a transverse resolution of 0.2 mm.

Ultrawideband Microwave Detection of Early-Stage Breast Cancer

Modeled Detection of a 2-mm Tumor

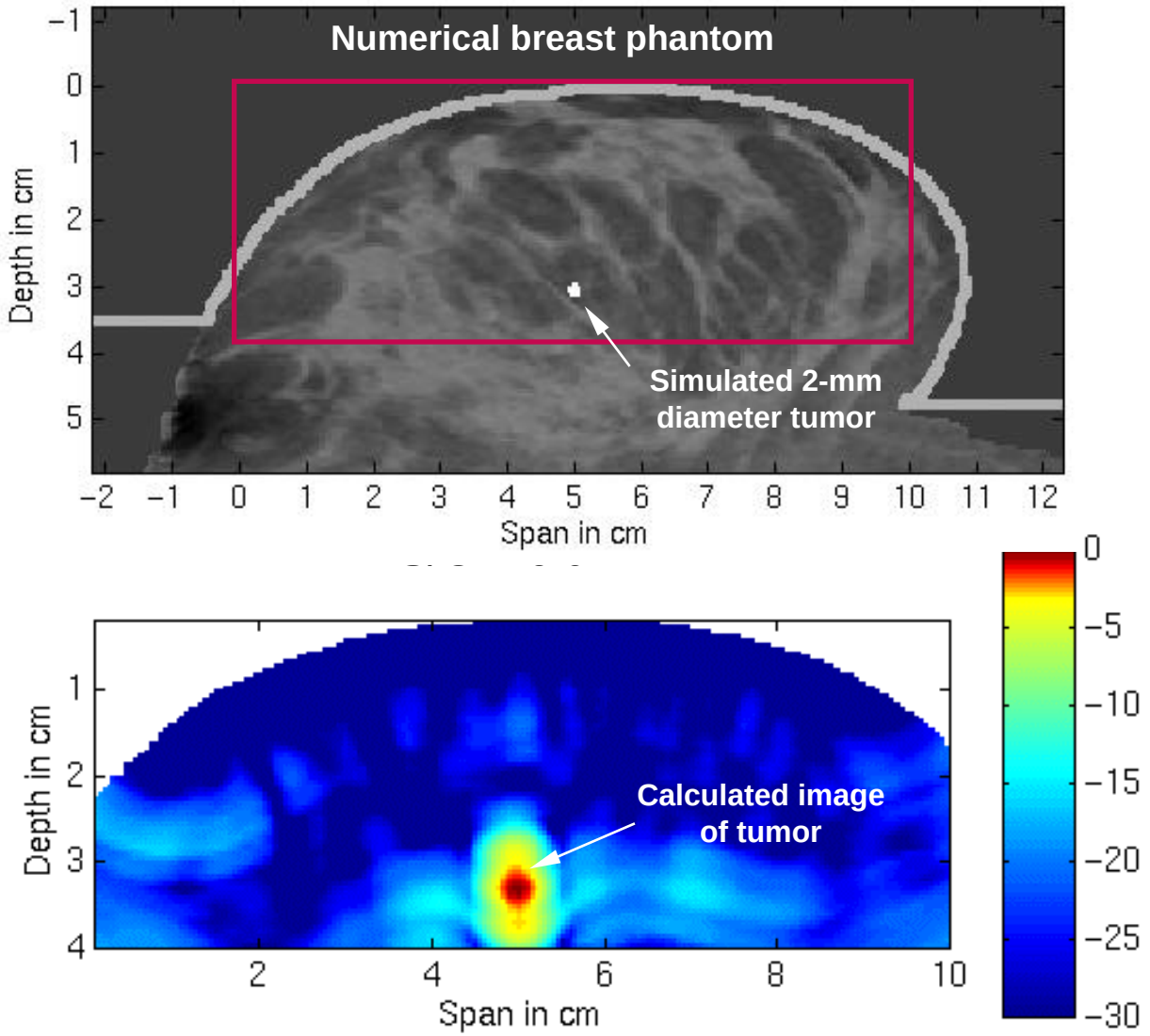

FDTD simulation of UWB microwave detection of a 2-mm-diameter malignant tumor embedded 3 cm within an MRI-derived numerical breast model. The cancer's signature is 15 to 30 dB stronger than the clutter due to the surrounding normal tissues. Source: Bond et al., *IEEE Trans. Antennas and Propagation,* 2003, pp. 1690–1705.

Ultrahigh-Speed Bandpass Digital Interconnects

Substrate Integrated Waveguides (SIW's)

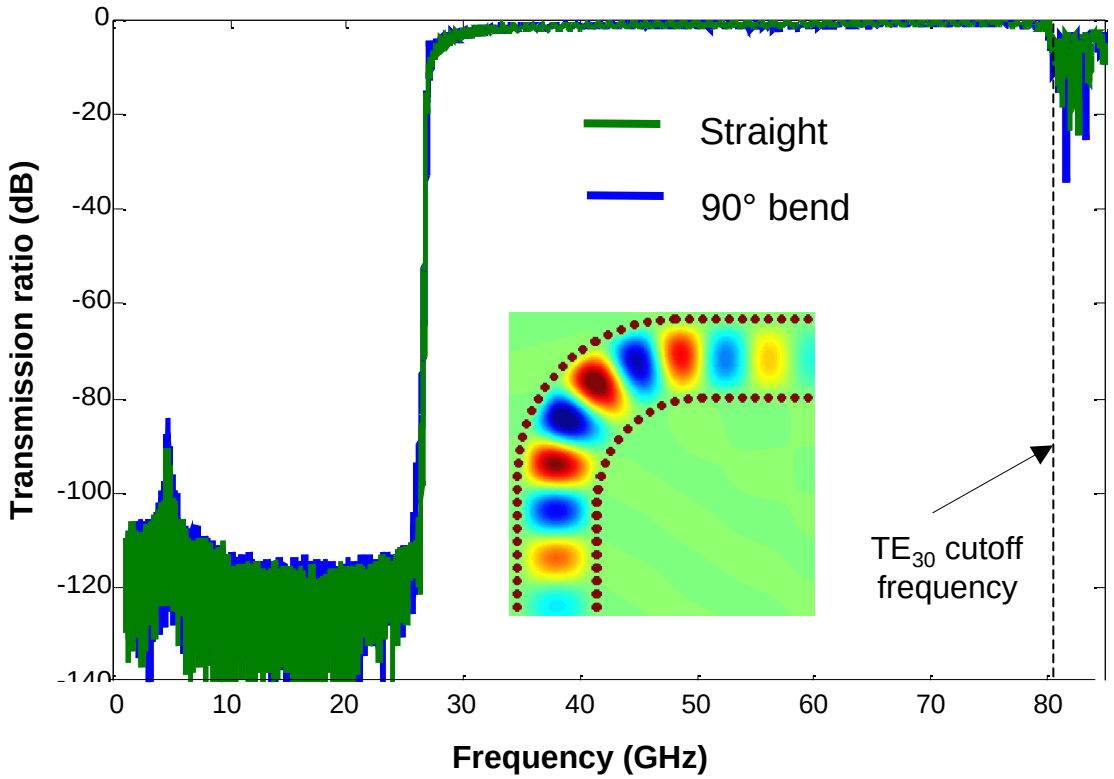

Both straight and bent SIW's exhibit100% bandwidths.

In this example, the passband is 27 to 81 GHz with negligible multimoding (as confirmed by measurements at Intel Corporation).

Source: Simpson et al, *IEEE Trans. MTT*, in press.

New Half-Width Folded SIW Has 115% Bandwidth Predicted by FDTD: 27 to 100 GHz

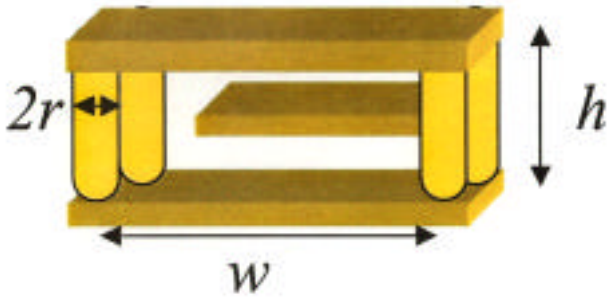

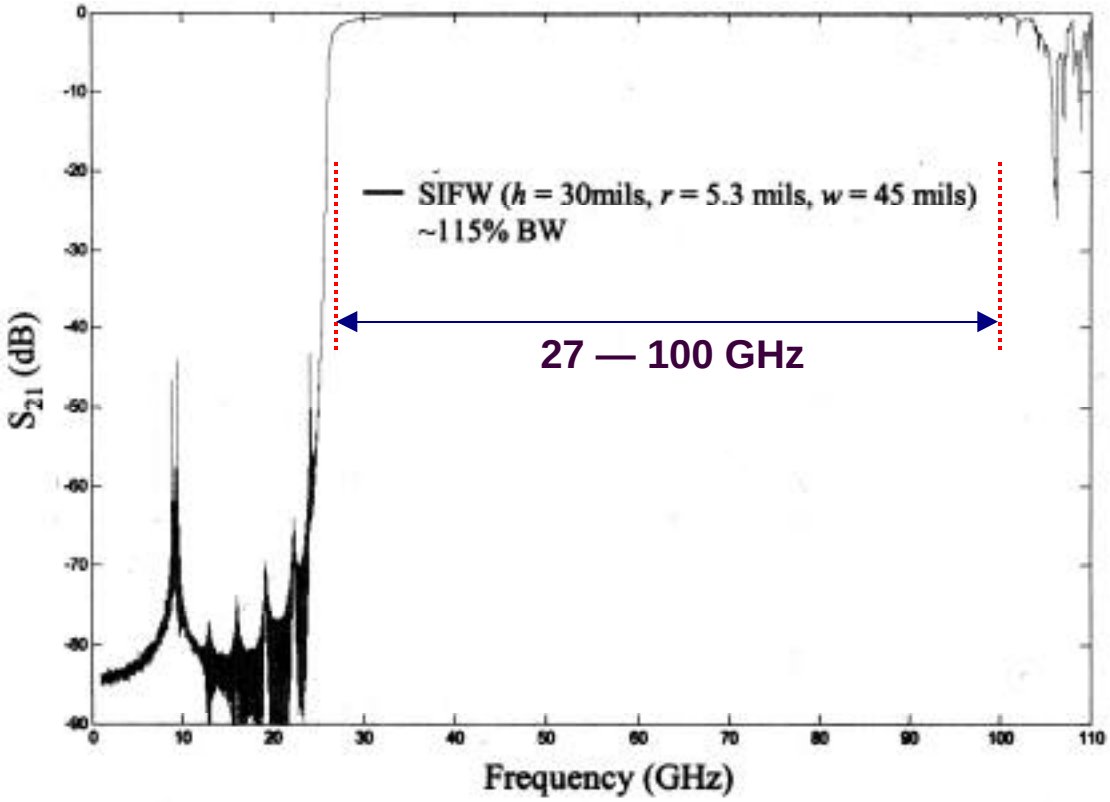

Micron / Nanometer Scale Photonic Devices
Category 1: Linear

Photonic Bandgap Defect Mode Cavities

Fabricated device: membrane microresonator in InGaAsP

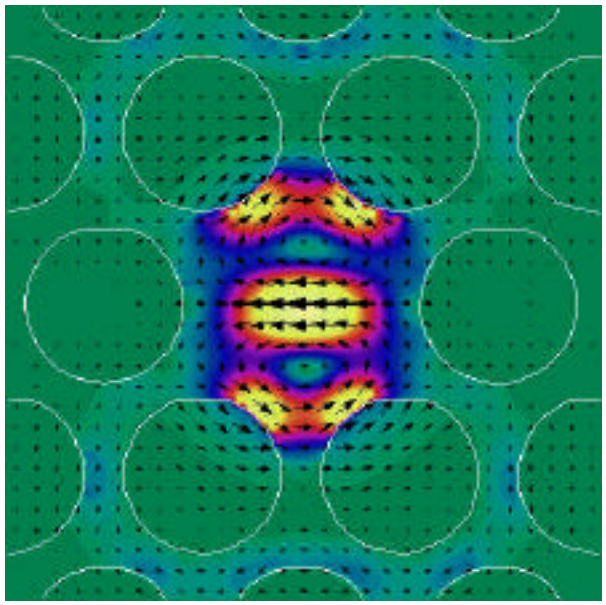

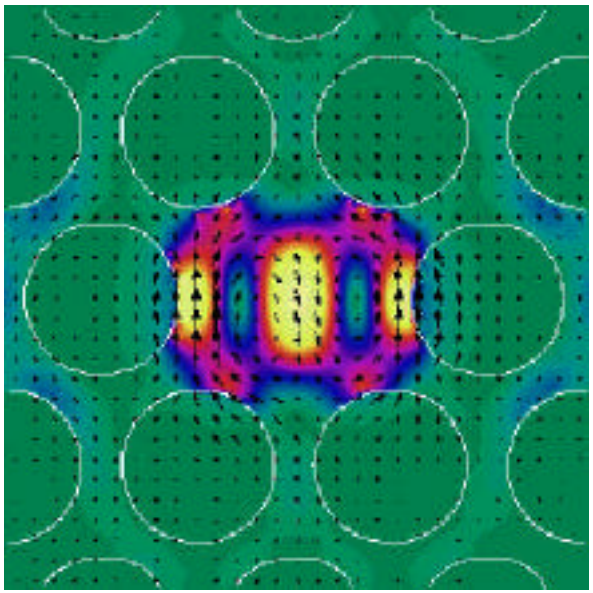

Images of degenerate microcavity modes in 2-D thin-film photonic crystal defect cavities

Source: E. Yablonovitch, UCLA

Photonic Bandgap Defect Mode Laser Cavities

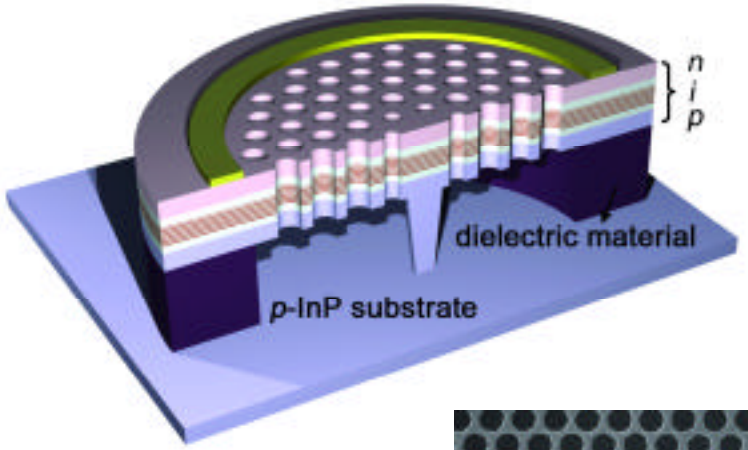

Schematic view

Electrically driven, single-mode, low-threshold-current photonic crystal microlaser operating at room temperature. Source: Park et al., *Science*, Sept. 3, 2004, pp. 1444–1447.

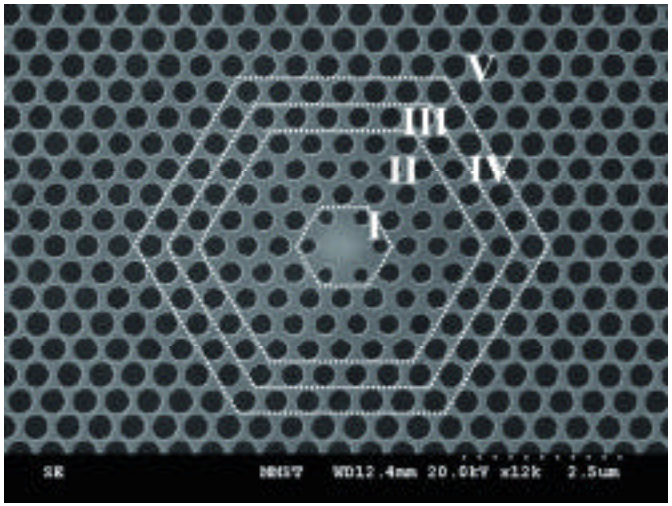

Top view of fabricated sample

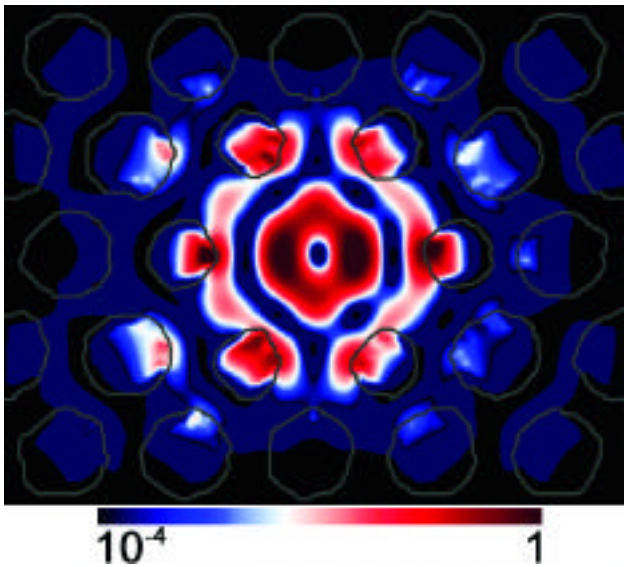

FDTD-calculated *E*-field intensity of monopole mode (log scale)

Laterally Coupled Photonic Disk Resonators

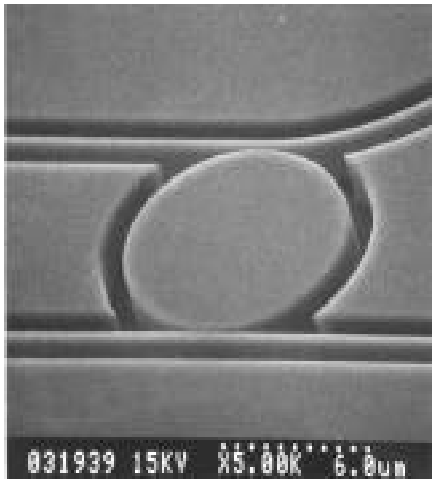

fabricated device

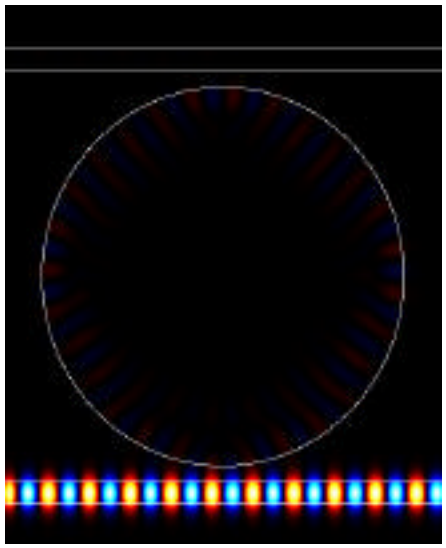

λ = 1.55 μm
(off resonance)

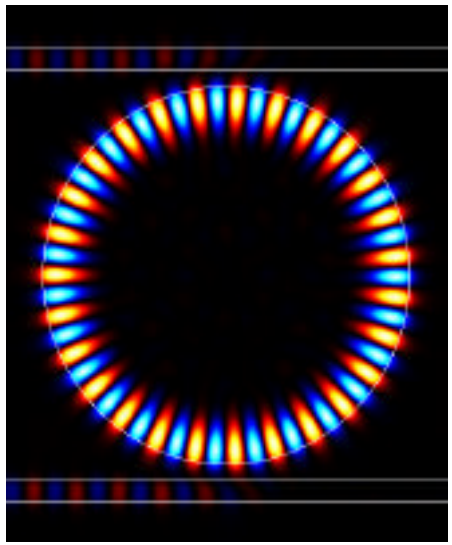

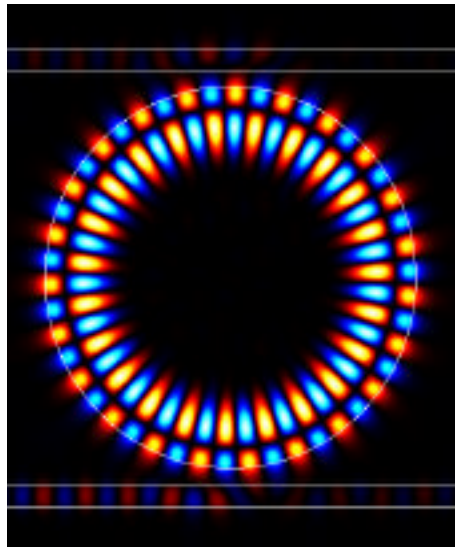

1st- and 2nd-order radial whispering gallery mode resonances

Source: S. C. Hagness, D. Rafizadeh, S. T. Ho, and A. Taflove, *IEEE J. Lightwave Tech.*, 1997.

Vertically Coupled Photonic Racetrack (Fully 3-D Model)

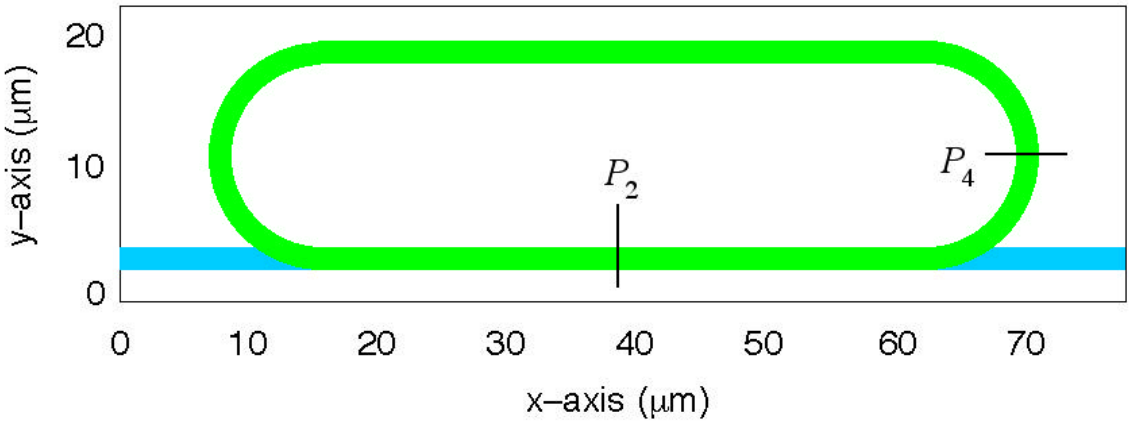

Plan view

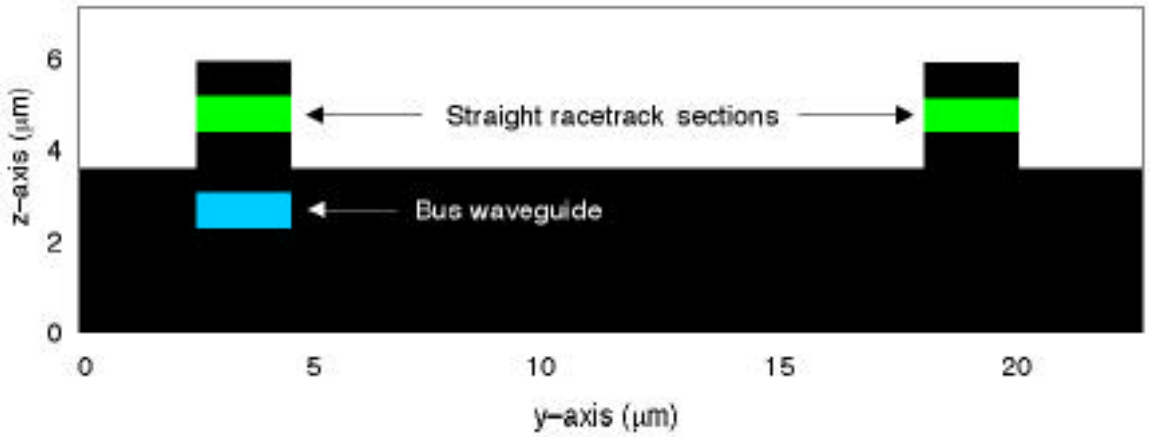

Vertical cross-section

Source: J. H. Greene and A. Taflove, *Optics Letters*, 2003.

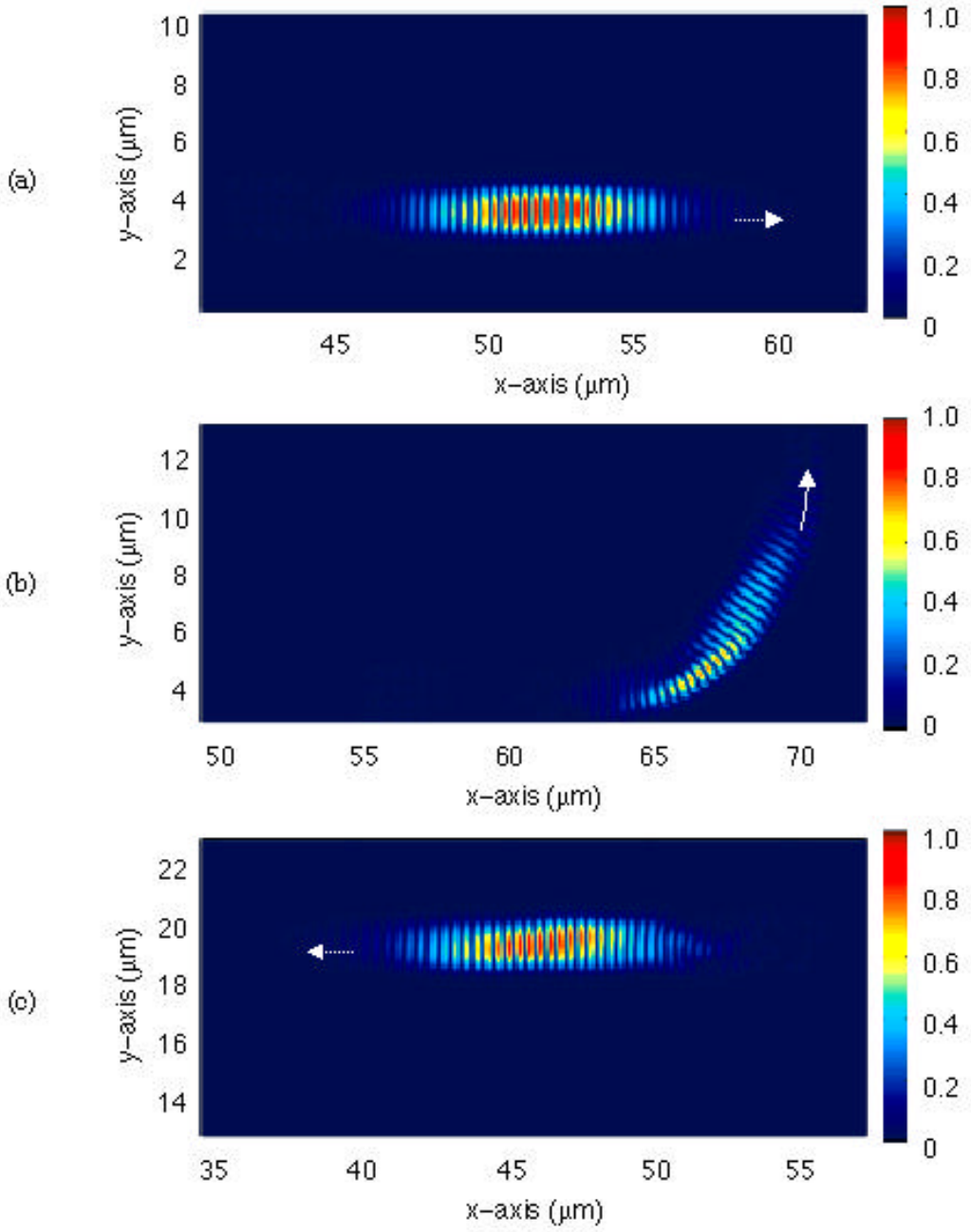

Pulse Propagation in the Vertically Coupled Racetrack

Vertical Cuts Showing Transient Multimoding

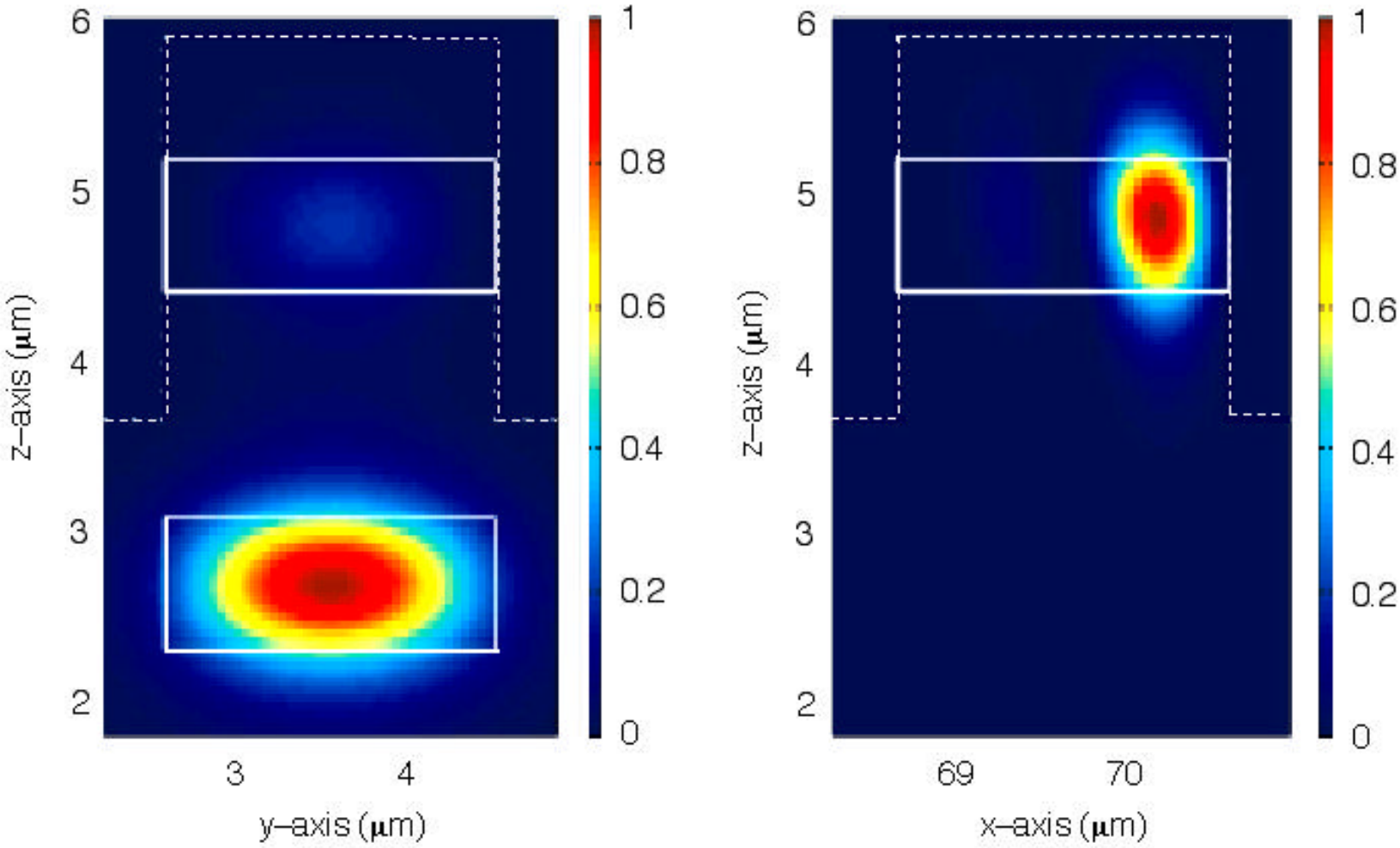

Nanoplasmonics: Enhanced Transmission Through a Sub-Micron Hole in a Gold Film

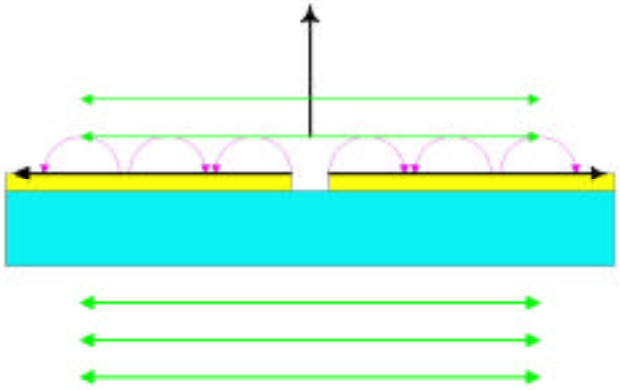

Gold film thickness = 100 nm
Hole diameter = 200 nm
Incident wavelength = 532 nm
Normal incidence

Experiment

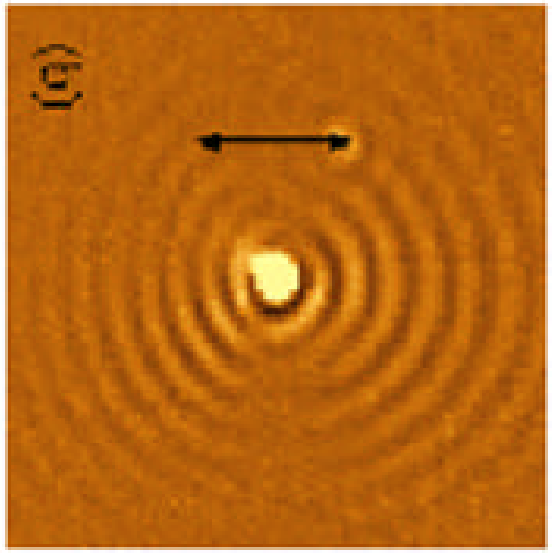

FDTD

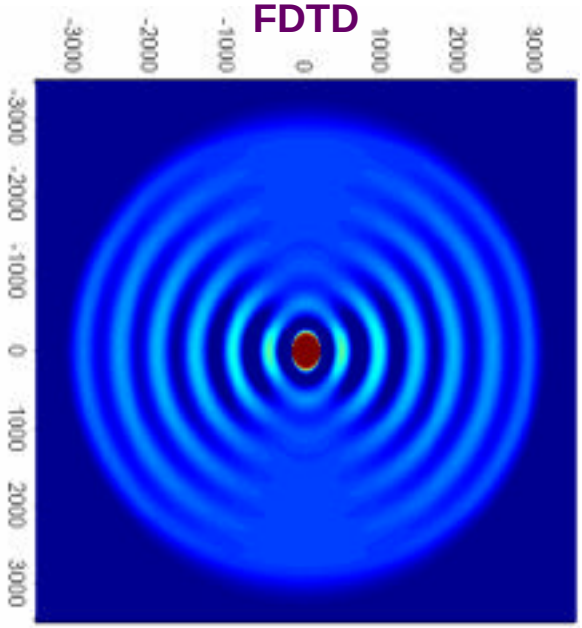

Source: L. Yin et al., *Applied Physics Letters* 85, 467 (2004)

Focusing Plasmonic Lens

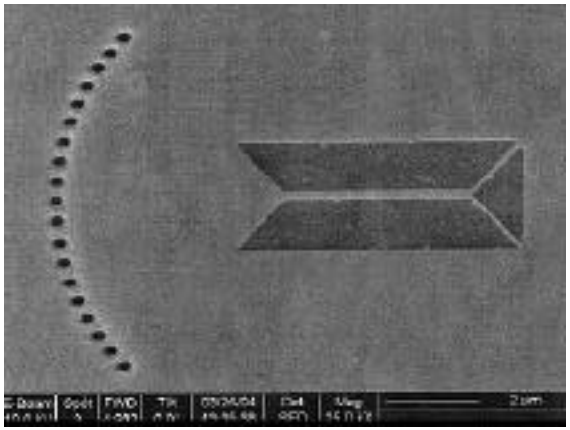

SEM photo

Source (left and bottom left images): L. Yin et al., *Nano Letters* 5, 1399 (2005).

Source (bottom right image): S-H. Chang

Experiment

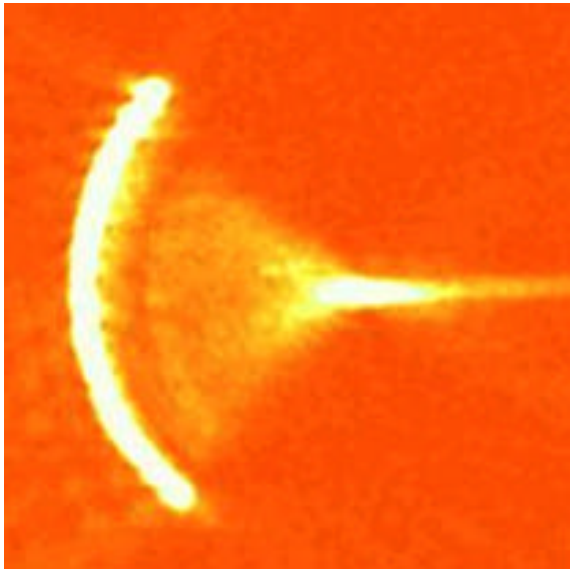

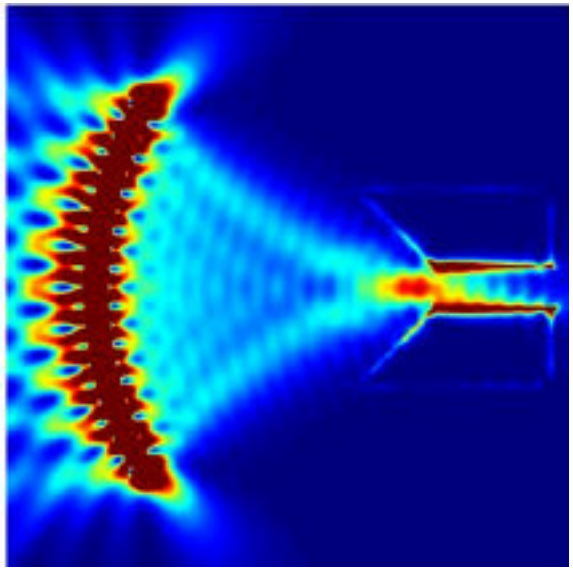

FDTD

Micron / Nanometer Scale Photonic Devices
Category 2: Macroscopic Nonlinearity

“Braided” Spatial Solitons in Glass

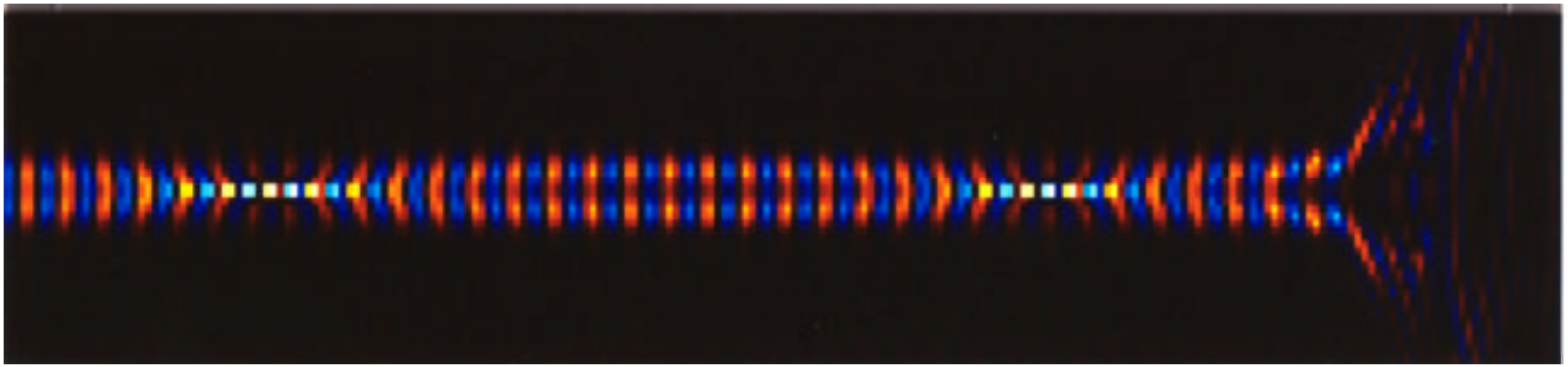

Source: R. Joseph and A. Taflove, *IEEE Photonics Technology Letters*, 1994.

Braiding Transitions to Divergence When the Width of Each Laser Beam is Sufficiently Narrow

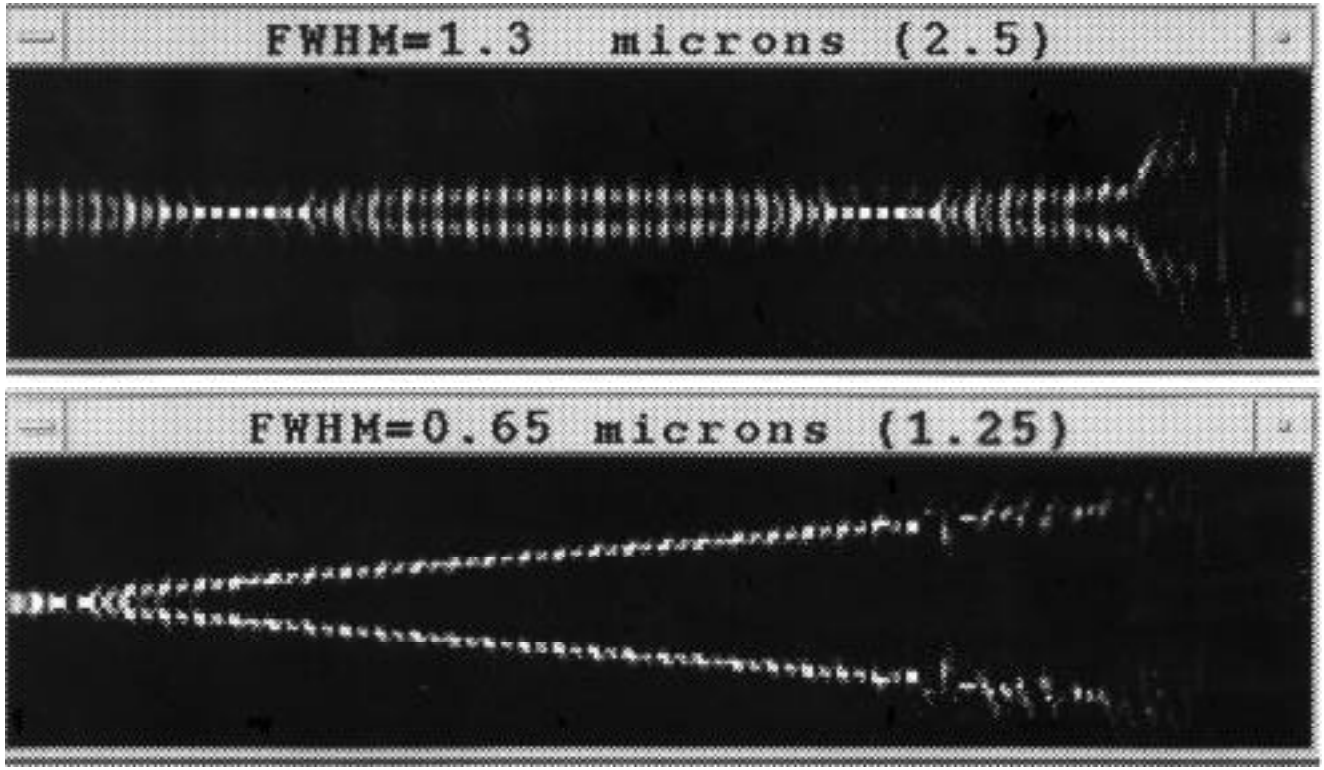

All-Optical Photonic Crystal Cross-Waveguide Switch

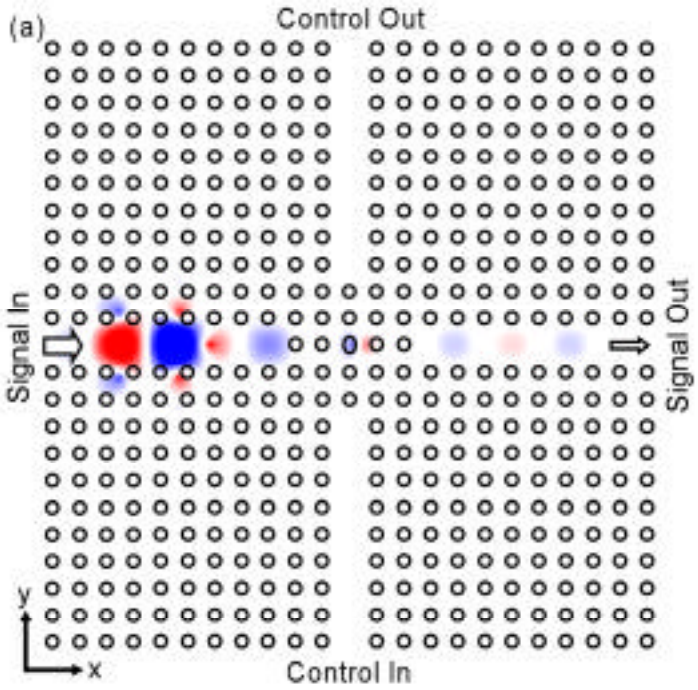

(a) control input is absent, yielding low signal output

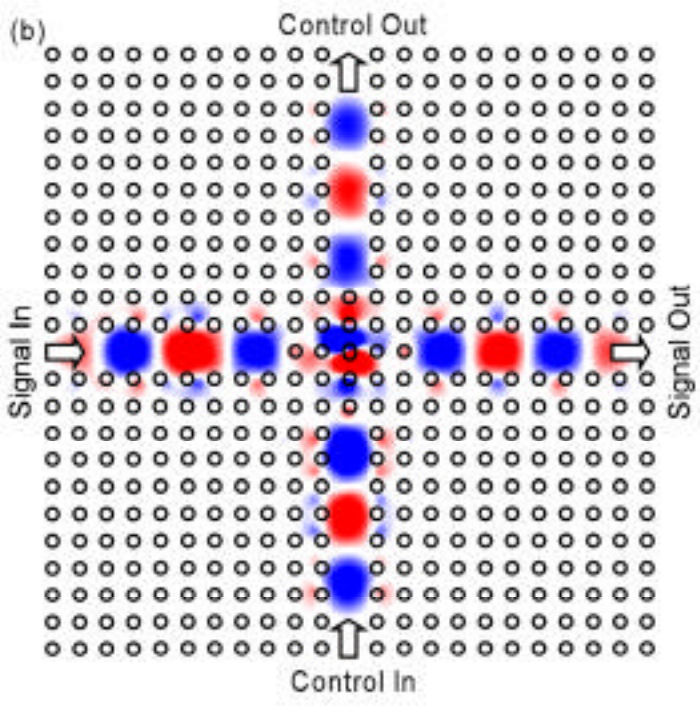

(b) control input is present, yielding high signal output

Source: Yanik et al., *Optics Letters*, 2003, pp. 2506–2508.

Micron / Nanometer Scale Photonic Devices
Category 3: Semiclassical Models

Four-Level, Two-Electron Model for ZnO

$$\frac{d^2 P_a}{dt^2} + \gamma_a \frac{dP_a}{dt} + \omega_a^2 P_a = k_a \left[N_3 - N_0 \right] E$$

$$\frac{d^2 P_b}{dt^2} + \gamma_b \frac{dP_b}{dt} + \omega_b^2 P_b = k_b \left[N_2 - N_1 \right] E$$

$$\frac{dN_3}{dt} = -\frac{N_3 (1 - N_2)}{\tau_{32}} - \frac{N_3 (1 - N_0)}{\tau_{30}} + \frac{1}{\hbar \omega_a} E \cdot \frac{dP_a}{dt}$$

$$\frac{dN_2}{dt} = \frac{N_3 (1 - N_2)}{\tau_{32}} - \frac{N_2 (1 - N_1)}{\tau_{21}} + \frac{1}{\hbar \omega_b} E \cdot \frac{dP_b}{dt}$$

$$\frac{dN_1}{dt} = \frac{N_2 (1 - N_1)}{\tau_{21}} - \frac{N_1 (1 - N_0)}{\tau_{10}} - \frac{1}{\hbar \omega_b} E \cdot \frac{dP_b}{dt}$$

$$\frac{dN_0}{dt} = \frac{N_3 (1 - N_0)}{\tau_{30}} + \frac{N_1 (1 - N_0)}{\tau_{10}} - \frac{1}{\hbar \omega_a} E \cdot \frac{dP_a}{dt}$$

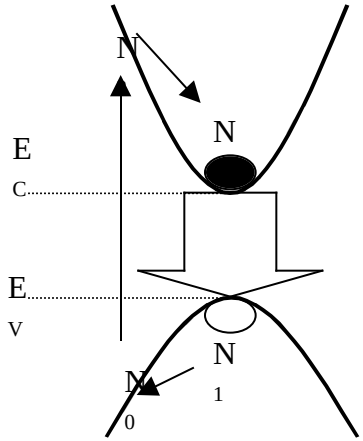

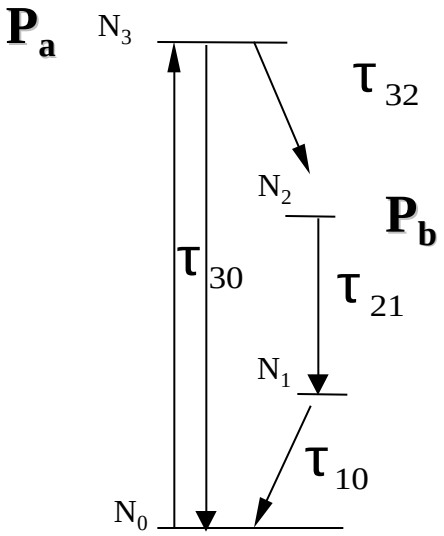

Source: S.-H. Chang and A. Taflove, *Optics Express*, 2004.

Pumping, Population Inversion, and Lasing

Populations n(t)

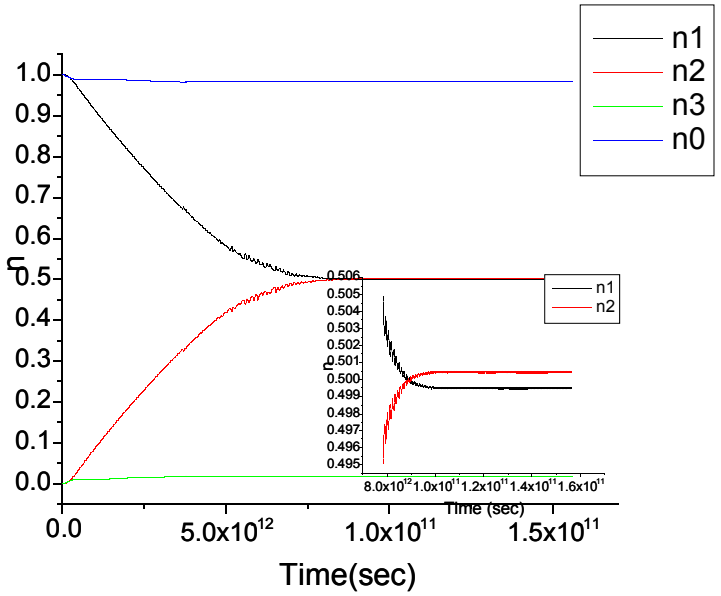

Pumping vs. lasing intensity

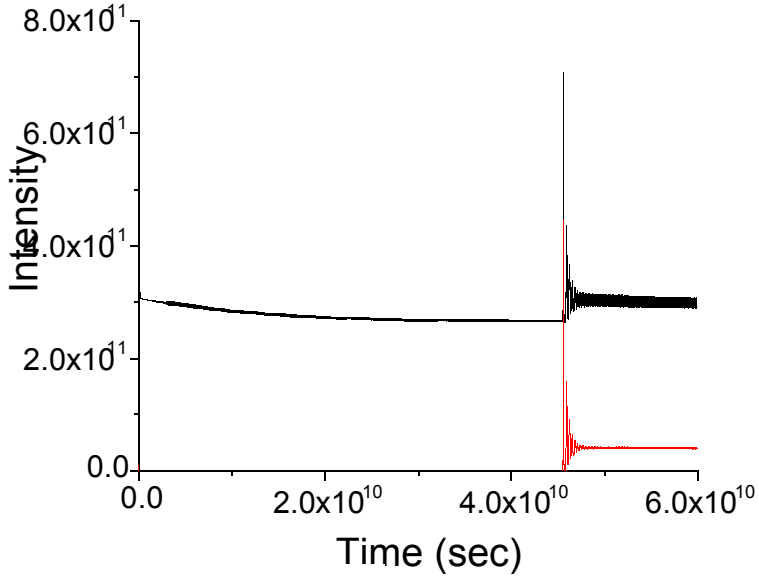

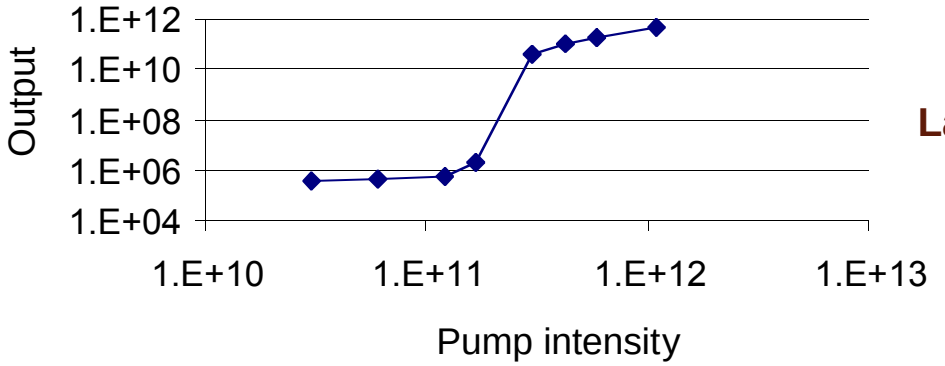

Lasing threshold

Lasing in a Random Clump of ZnO Particles

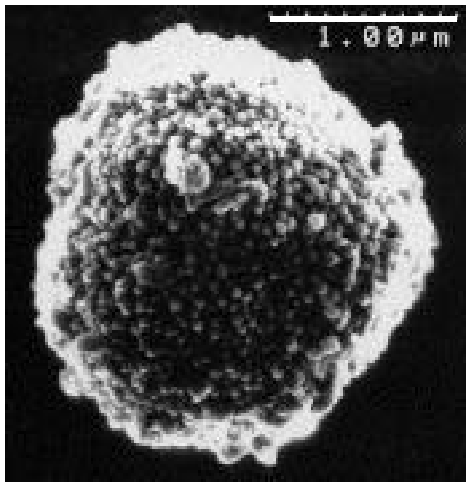

size ~ 1.7 μm
Contains ~ 20,000 particles

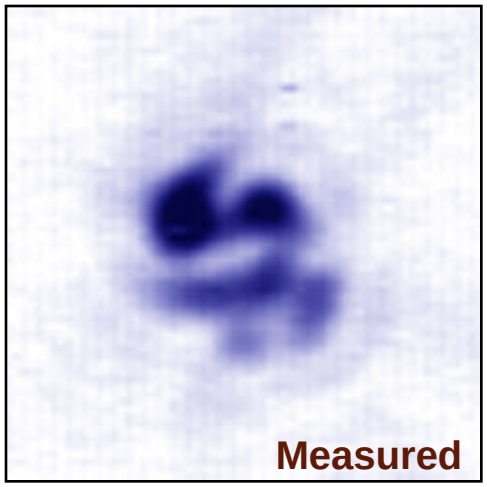

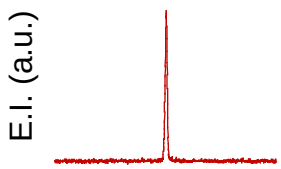

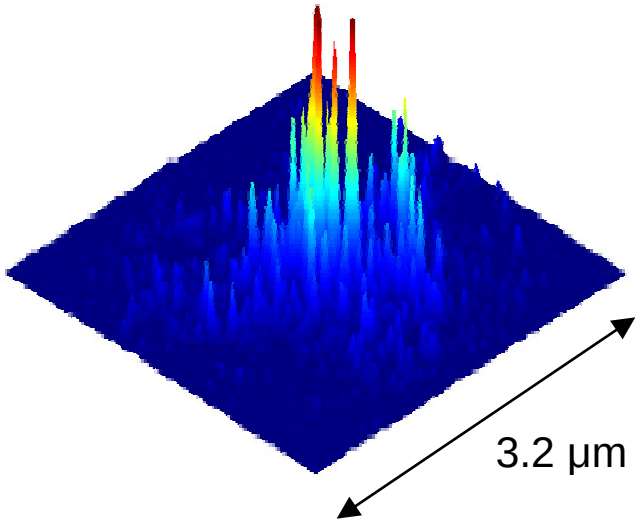

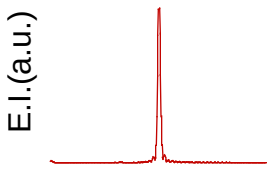

2-D FDTD model

Source: H. Cao et al., *Physical Review Letters,* 2000.

Biophotonics

FDTD / PSTD Biophotonics Thrust Areas

- Optical detection of early-stage epithelial cancers (colon, lung, esophagus, cervix)
- Ultramicroscopy of individual living cells to investigate physiological processes
- Optical propagation through millimeter-scale-thick living tissues

What is the Difference Between These Two Groups of Human Cells (observed using conventional microscopy)?

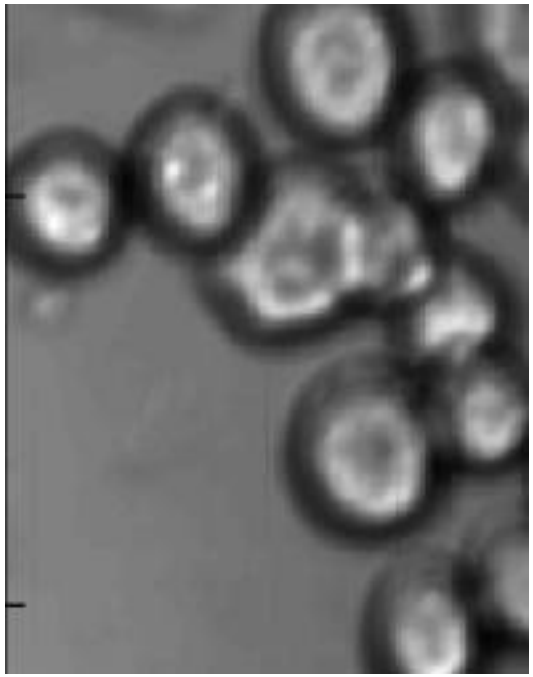

Healthy cells

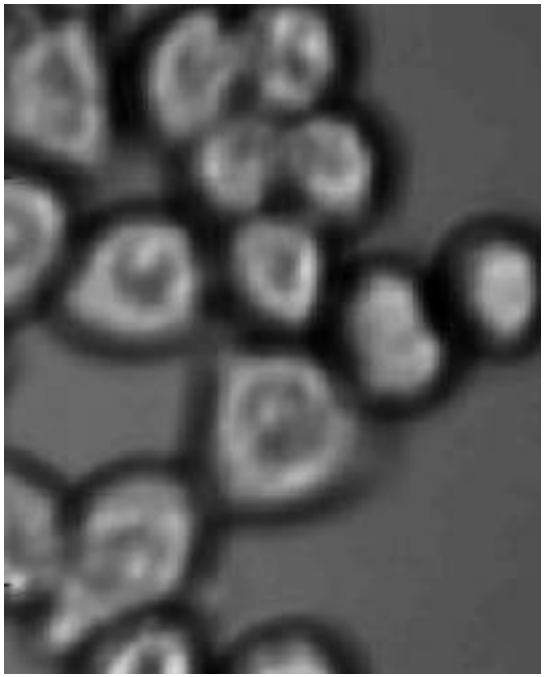

Cells near death

Backscattering Spectroscopy

Our FDTD modeling has shown that observing the spectrum of retro-reflected light from living tissues yields much greater information regarding the health of these tissues than existing diagnostic techniques.

Backscattering Detection of Nanoscale Features

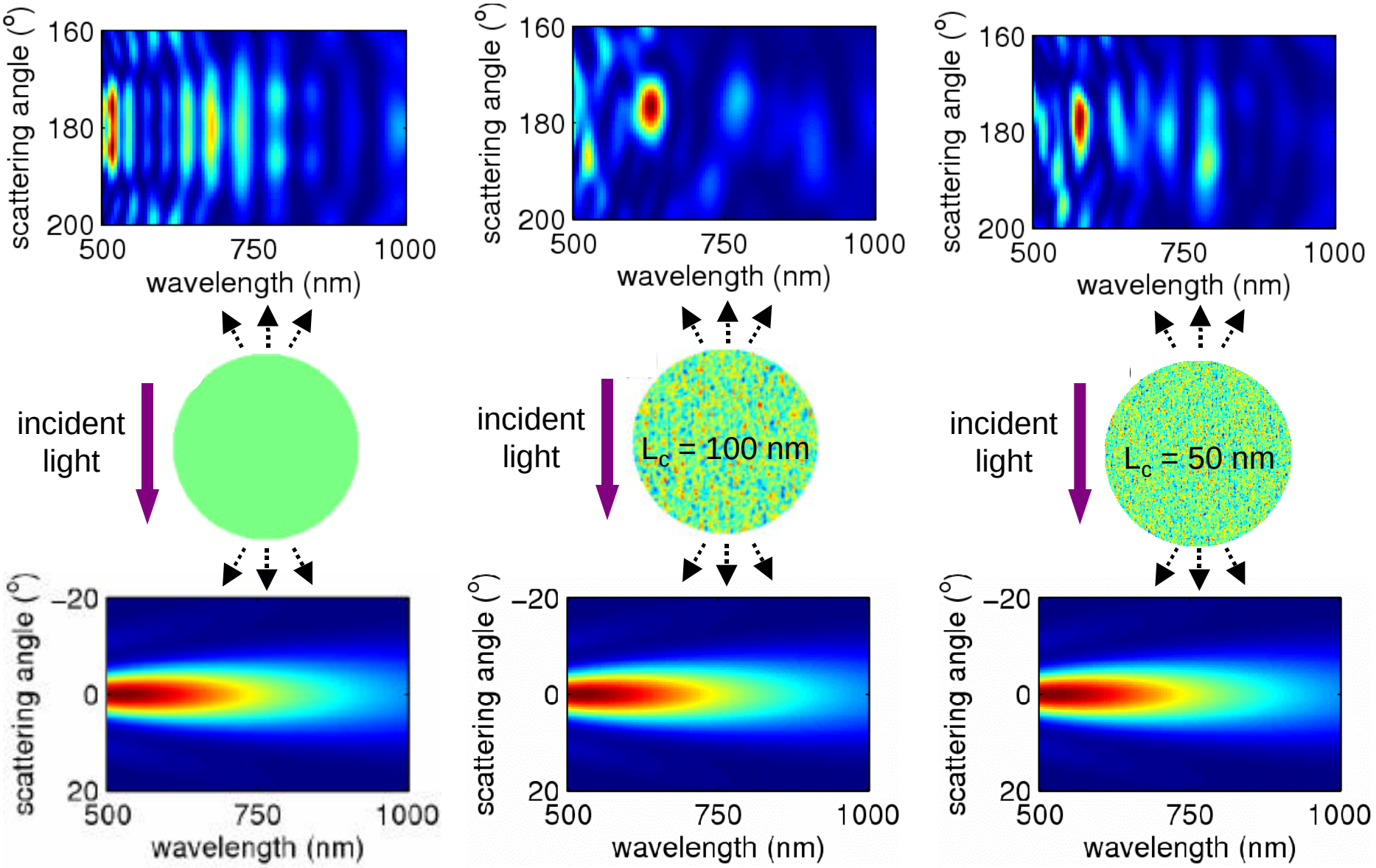

Emerging Clinical Application

My Northwestern University colleagues and collaborators, Profs. Vadim Backman and Xu Li, are applying this idea to develop extraordinarily sensitive and accurate tests for pre-cancerous conditions in human epithelial tissues such as the colon.

Bulk Backscattering Spectral Changes Are Observed Far Earlier Than Any Currently Known Histologic or Molecular Markers of Precancerous Conditions in Colon Tissues

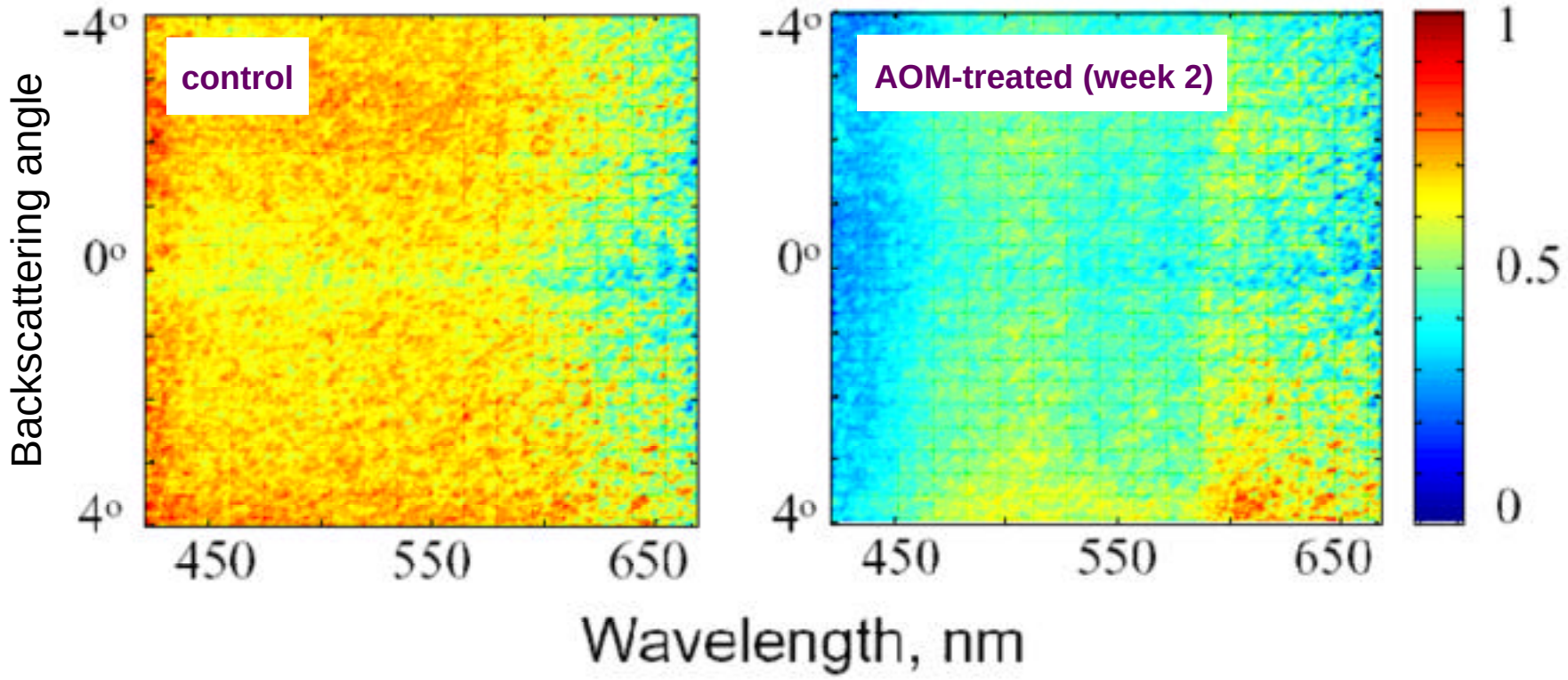

Source: ***Gastroenterology*, 126, 1071-1081 (2004).**

Our Current Work: Backscattering Spectroscopic Microscopy On a Pixel-by-Pixel Basis

Using FDTD simulations to guide experiments, we are pushing this concept even further to acquire the backscattered spectra of individual pixels of a microscope image.

This will allow monitoring of the physiological processes involved in the progression of precancerous conditions in living human cells.

First, We Demonstrated Agreement of Measured and FDTD-Calculated Backscattering Microscope Images

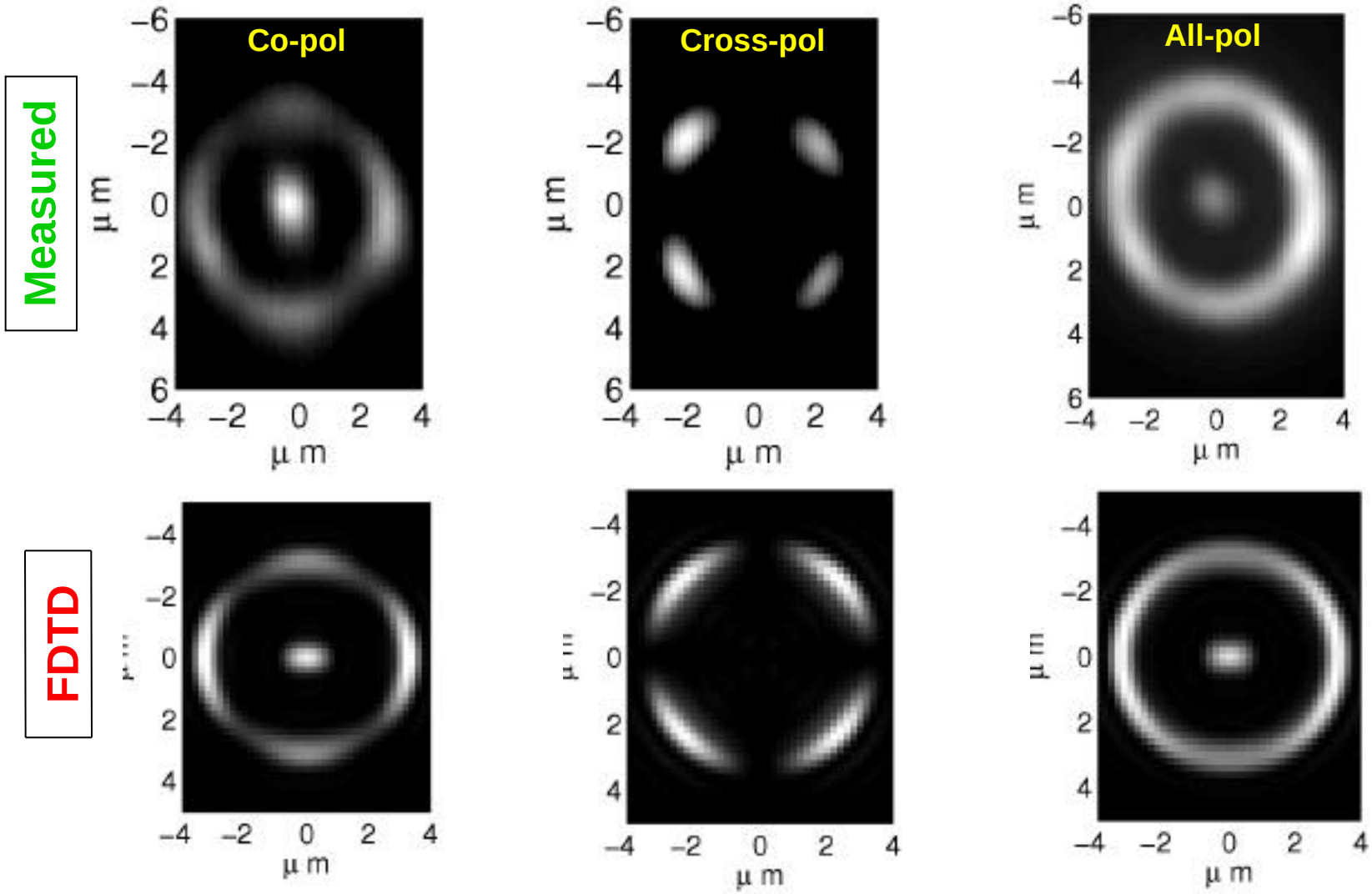

Next, We Applied FDTD to Calculate the Spectra of Individual Pixels of Backscattered Microscope Images of Various Layered Media Having Lateral Inhomogeneities Near the Diffraction Limit

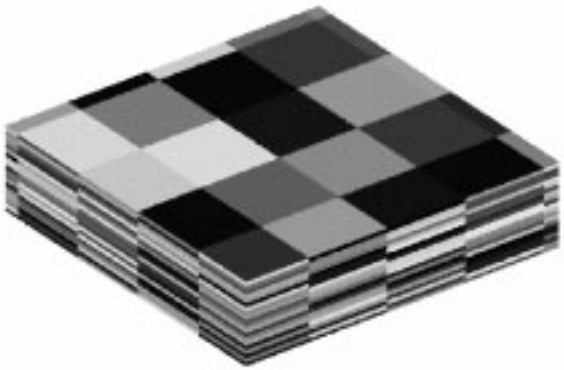

Modeled structure

FDTD-calculated image

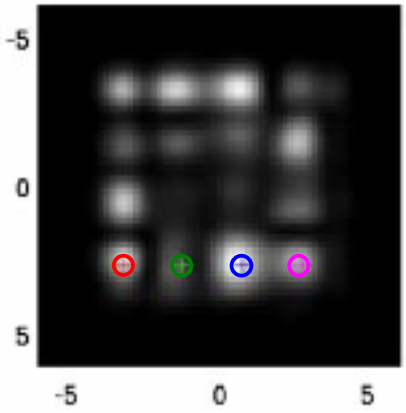

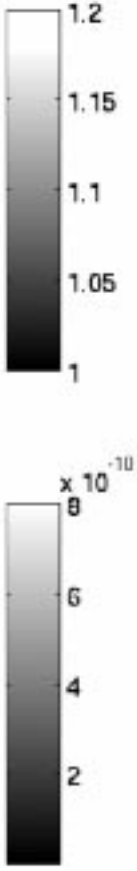

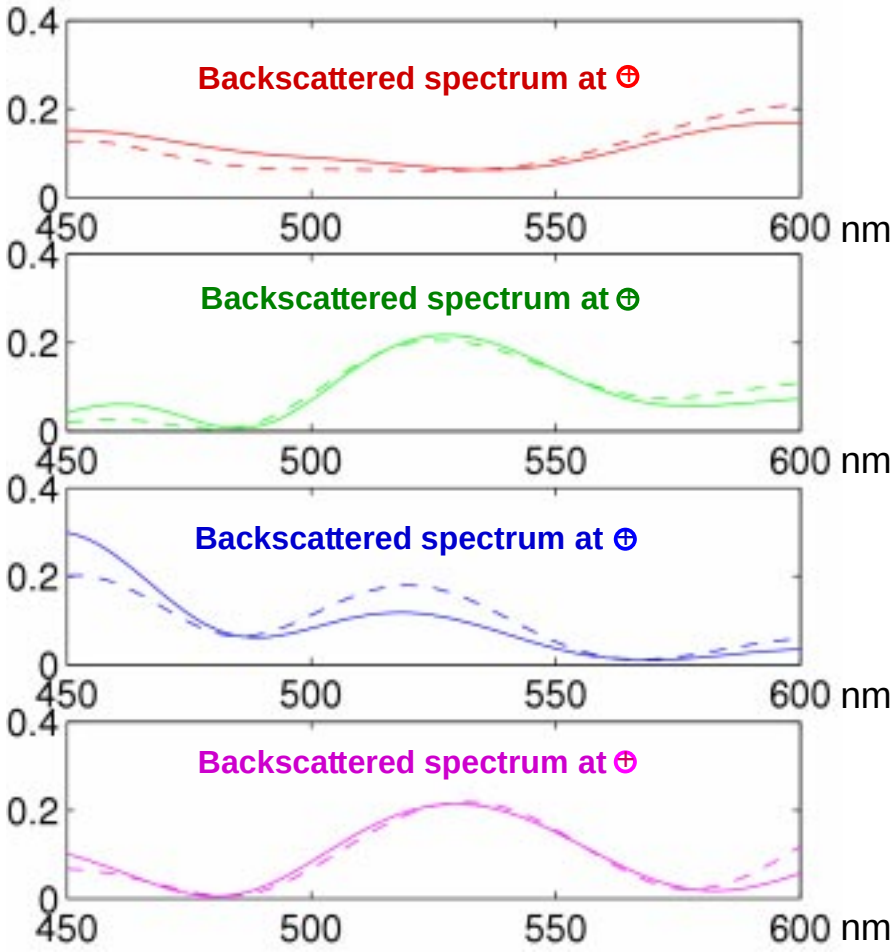

Finally, We Designed a Microscope System to Acquire Pixel-by-Pixel Backscattering Spectra of Individual Biological Cells

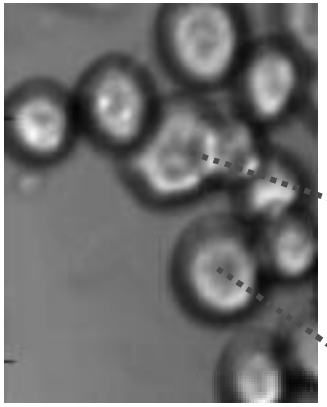

Backscattering microscope intensity image of normal HT-29 cells

Same, but the HT-29 cells are treated with sulindac sulfide

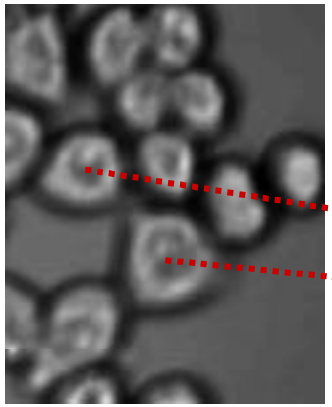

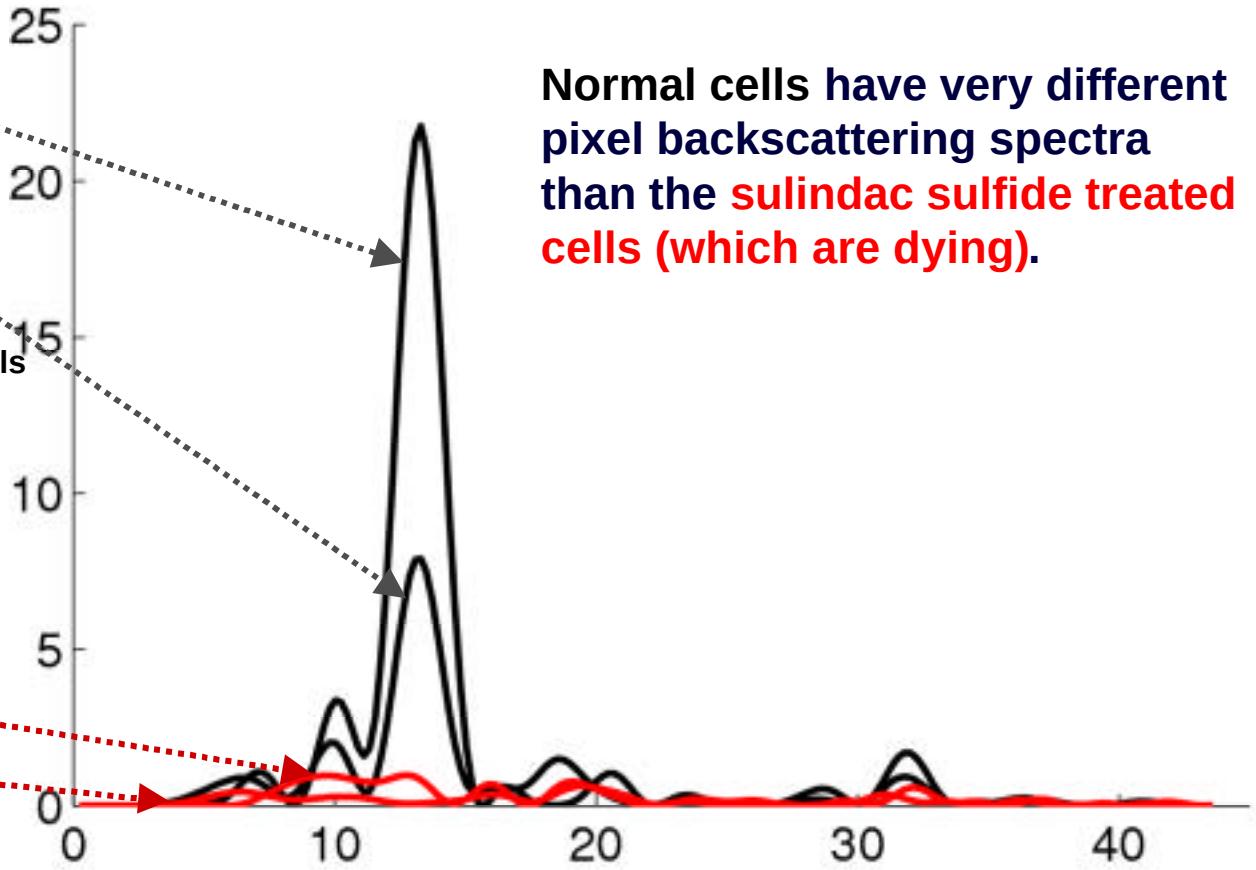

Single-pixel backscattering spectra

Normal cells have very different pixel backscattering spectra than the sulindac sulfide treated cells (which are dying).

PSTD Modeling of Clusters of Cells

We are applying PSTD modeling to better understand the interaction of light with large clusters of living cells.

We are particularly interested in direct backscattering, which conveys much information regarding tissue health.

Validation of Fourier-Basis PSTD for Scattering by a Single Sphere

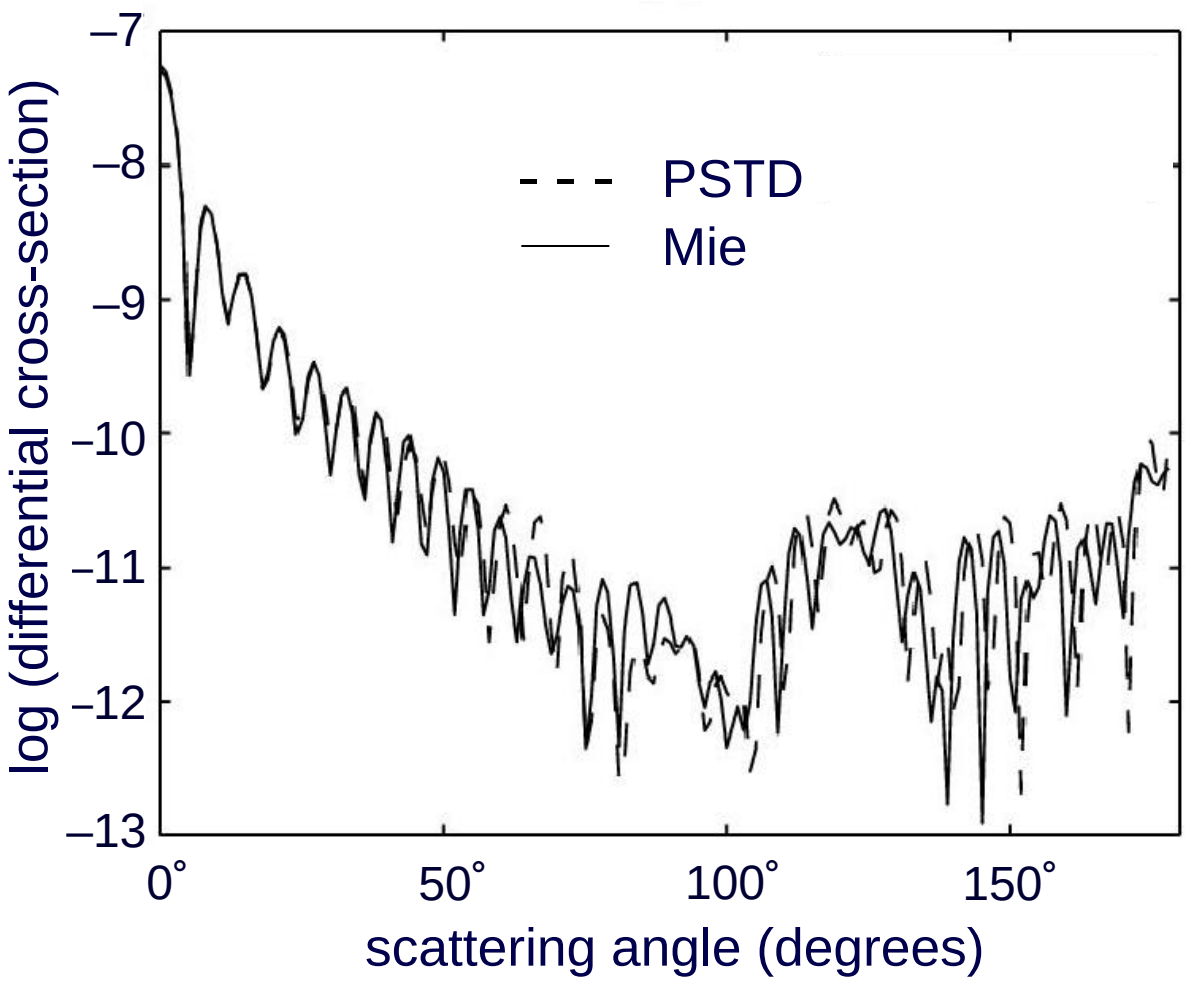

Source: Tseng et al., *Radio Science*, in press.

Validation of Fourier-Basis PSTD for Scattering by a 20-μm-Diameter Cluster of 19 Dielectric Spheres

19 spheres, each d = 6 μm and n = 1.2

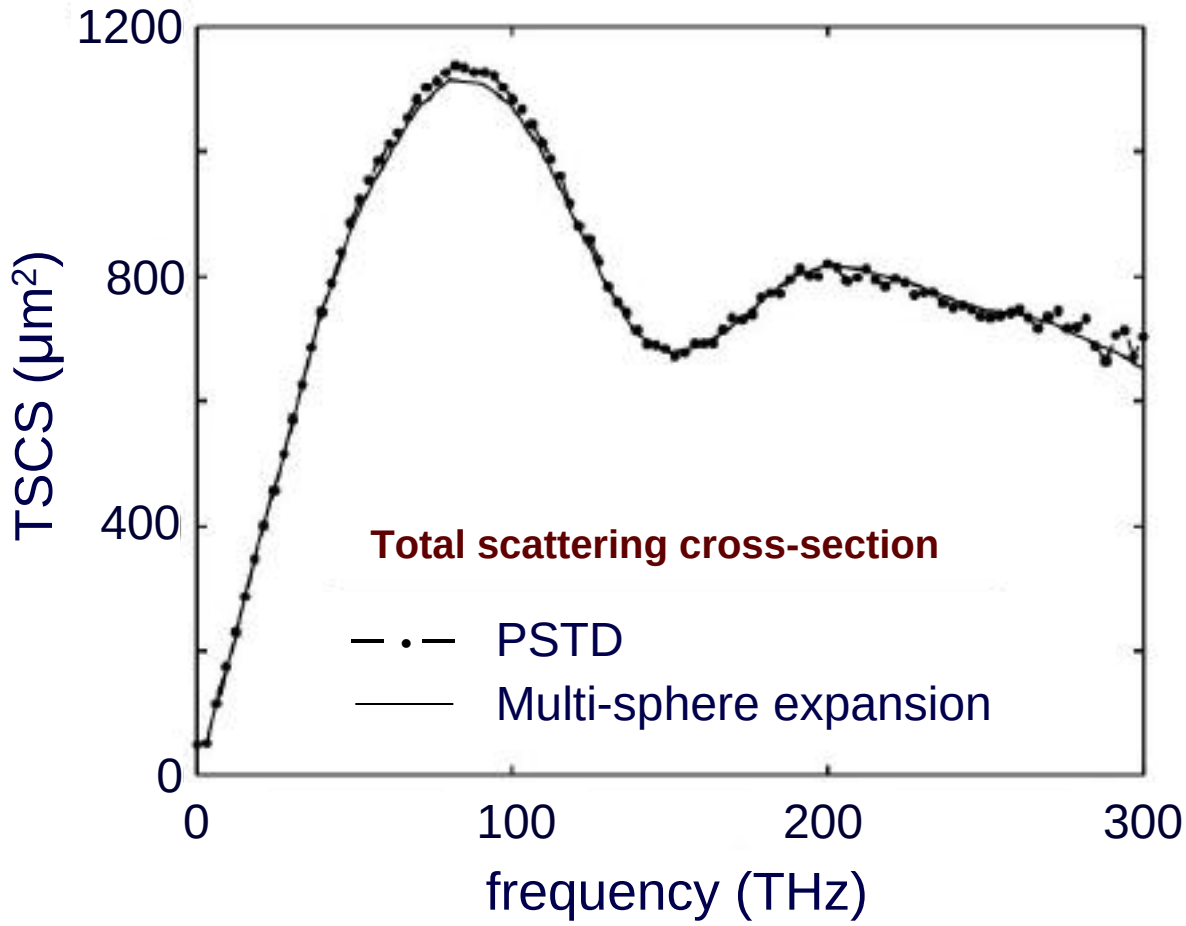

PSTD-Calculated Total Scattering Cross-Section of a 25-μm-Diameter Cluster of 192 Dielectric Spheres

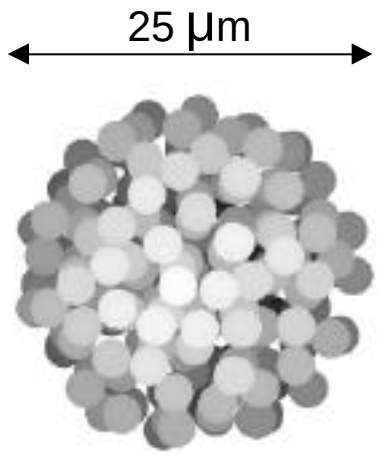

192 spheres, each d = 3 μm and n = 1.2

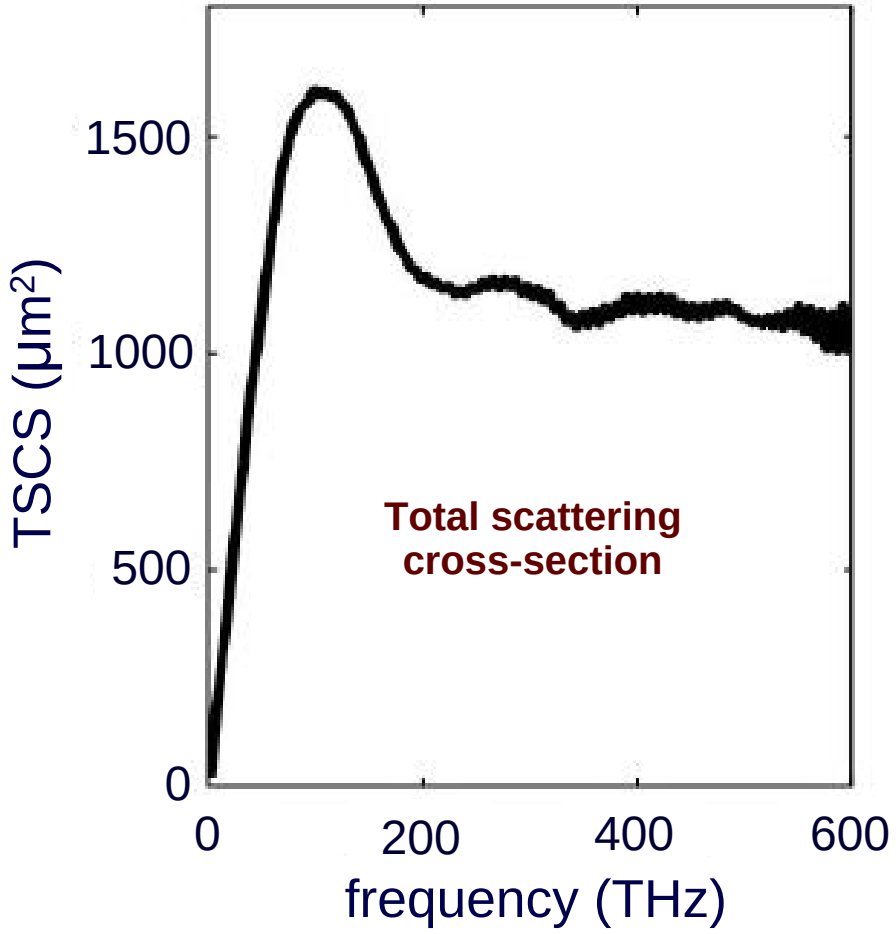

Identification of the Component Sphere Size in the 192-Sphere Cluster Via Cross Correlation

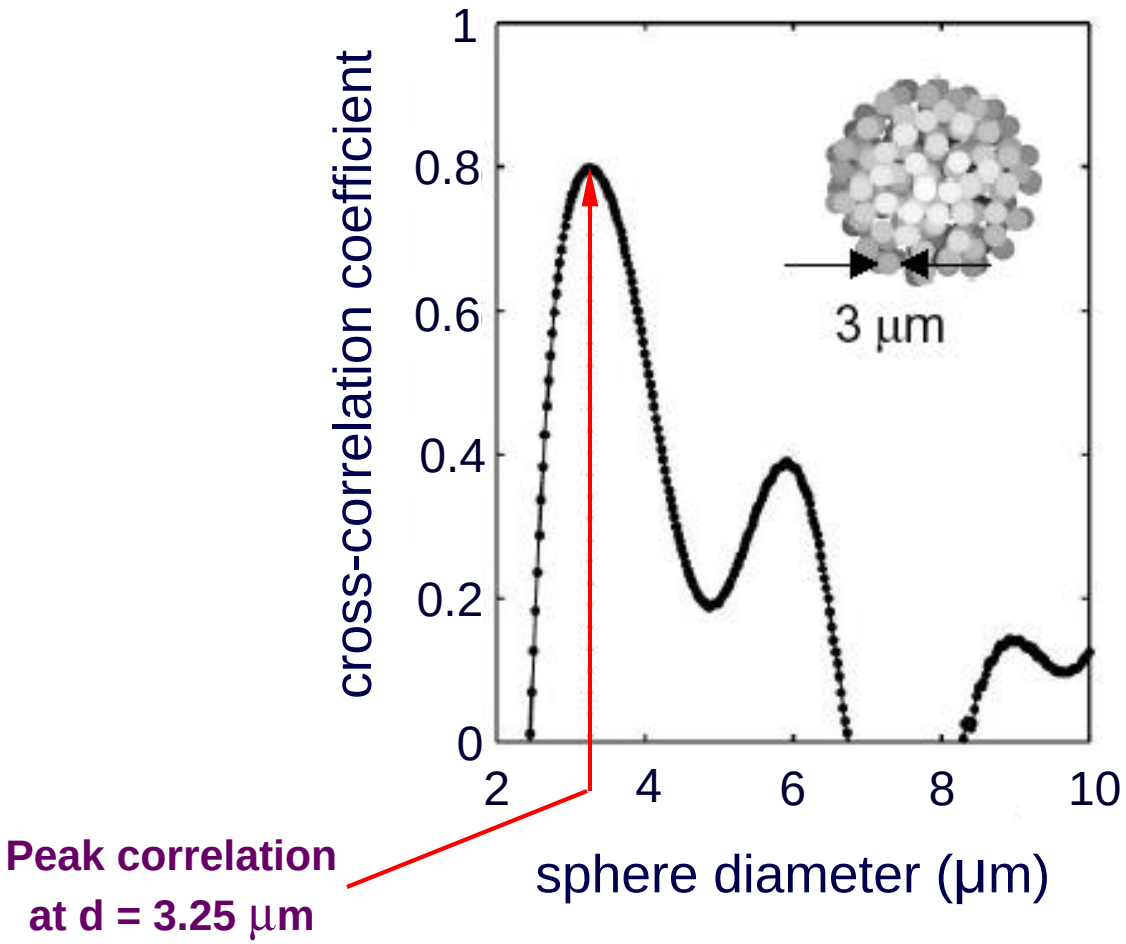

Future Prospects

- Nanophotonics, including as many quantum effects as we can muster. Ultimately, achieve a combination of quantum and classical electrodynamics.
- Biophotonics, especially as applied to the early-stage detection of dread diseases such as cancer.

My Personal Journey

I've been privileged to participate in the advancement of FDTD theory, techniques, and applications over the past 35 years.

It is very gratifying to see the current general widespread usage of FDTD for engineering and science applications that could not have been envisioned back in the1970's and 1980's.

Thanks for inviting me!